

# ELEC 677: Training Convnets Lecture 5

**Ankit B. Patel**

*Baylor College of Medicine (Neuroscience Dept.)*

*Rice University (ECE Dept.)*

09-20-2016

# Administrivia

- Please start Assignment #1 ASAP!!!

# Latest News

# Professor Richards-Kortum Named MacArthur Fellow



# ILSVRC 2016 Results Are Available

## Task 2a: Classification+localization with provided training data

Ordered by localization error

Team name	Entry description	Localization error	Classification error
Trimp-Soushen	Ensemble 3	0.077087	0.02991
Trimp-Soushen	Ensemble 4	0.077429	0.02991
Trimp-Soushen	Enaemble 2	0.077668	0.02991
Trimp-Soushen	Ensemble 1	0.079068	0.03144
Hikvision	Ensemble of 3 Faster R-CNN models for localization	0.087377	0.03711
Hikvision	Ensemble of 4 Faster R-CNN models for localization	0.087633	0.03711
NUIST	prefer multi box prediction with refine	0.090593	0.03461
NUIST	prefer multi class prediction	0.094058	0.03351

## Task 3c: Object detection/tracking from video with provided training data

Team name	Entry description	mean AP
CUVideo	4-model ensemble	0.558557
NUIST	cascaded region regression + tracking	0.548781
CUVideo	Single GBD-Net	0.526137
MCG-ICT-CAS	ResNet101+ResNet200 models for detection, optical flow for tracking, Coherent tublet reclassification++, MDNet tracking	0.488832

## Task 3a: Object detection from video with provided training data

Ordered by number of categories won

Team name	Entry description	Number of object categories won	mean AP
NUIST	cascaded region regression + tracking	10	0.808292
NUIST	cascaded region regression + tracking	10	0.803154
CUVideo	4-model ensemble with Multi-Context Suppression and Motion-Guided Propagation	9	0.767981
Trimp-Soushen	Enaemble 2	1	0.709651

## Scene Classification (Scene)<sup>(top)</sup>

Team name	Entry description	Top-5 classification error
Hikvision	Model D	0.0901
Hikvision	Model E	0.0908
Hikvision	Model C	0.0939
Hikvision	Model B	0.0948
MW	Model ensemble 2	0.1019
MW	Model ensemble 3	0.1019
MW	Model ensemble 1	0.1023
Hikvision	Model A	0.1026
Trimp-Soushen	With extra data.	0.103
Trimp-Soushen	Ensemble 2	0.1042

# Bay Area Deep Learning School

## **Slides**

<http://www.bayareadlschool.org/schedule>

## **Video for Day 1**

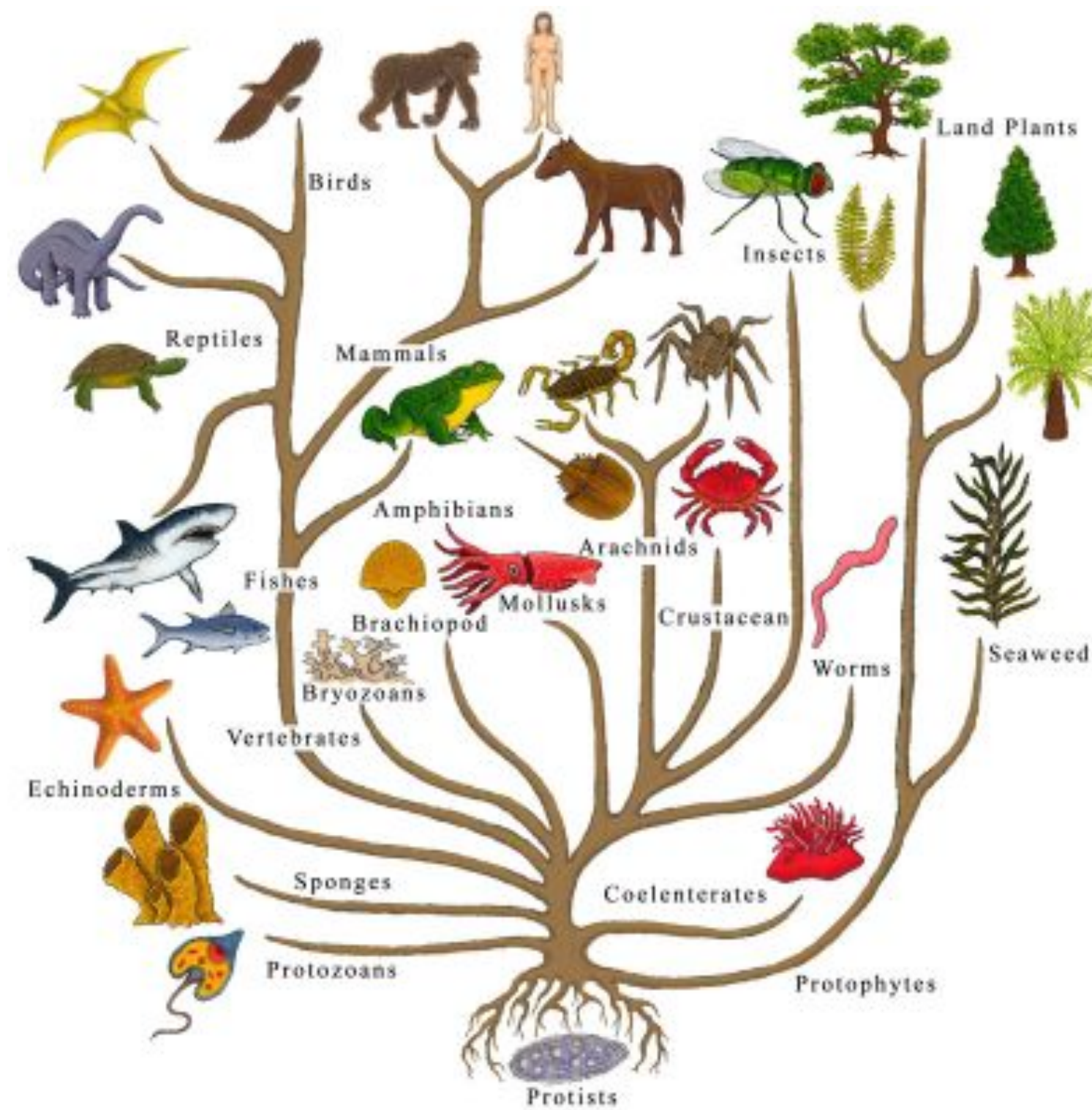
<https://www.youtube.com/watch?v=eyovmAtoUx0>

## **Video for Day 2**

<https://www.youtube.com/watch?v=9dXiAecyJrY>

# Species of Convnets

# Evolutionary Biology



*A mostly complete chart of*

# Neural Networks

©2016 Fjodor van Veen - [asimovinstitute.org](http://asimovinstitute.org)

-  Backfed Input Cell
-  Input Cell
-  Noisy Input Cell
-  Hidden Cell
-  Probabilistic Hidden Cell
-  Spiking Hidden Cell
-  Output Cell
-  Match Input Output Cell
-  Recurrent Cell
-  Memory Cell
-  Different Memory Cell
-  Kernel
-  Convolution or Pool

Perceptron (P)



Feed Forward (FF)



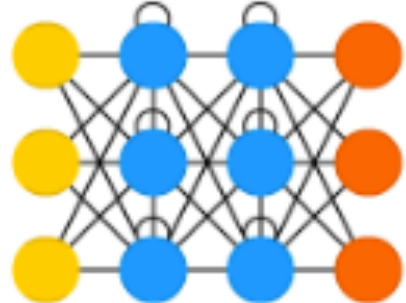
Radial Basis Network (RBF)



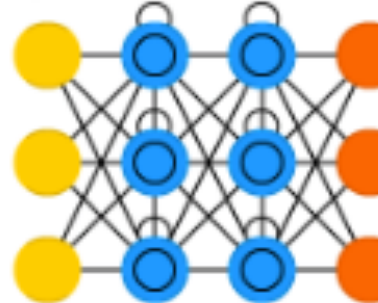
Deep Feed Forward (DFF)



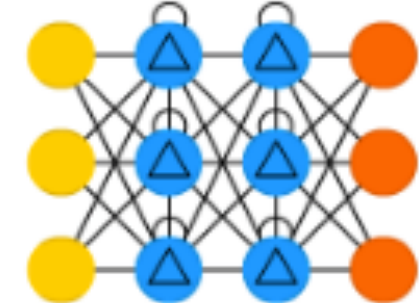
Recurrent Neural Network (RNN)



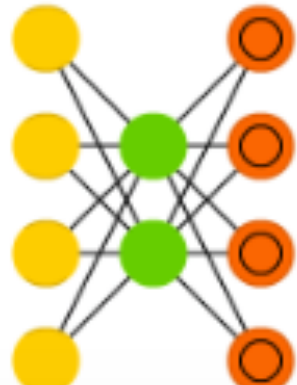
Long / Short Term Memory (LSTM)



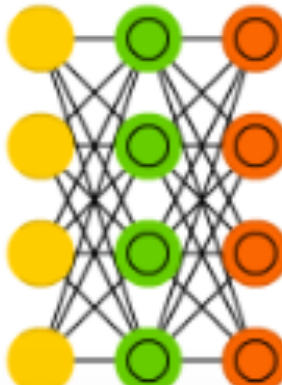
Gated Recurrent Unit (GRU)



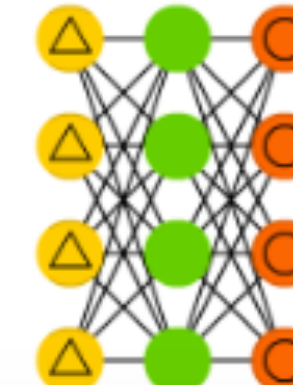
Auto Encoder (AE)



Variational AE (VAE)



Denoising AE (DAE)

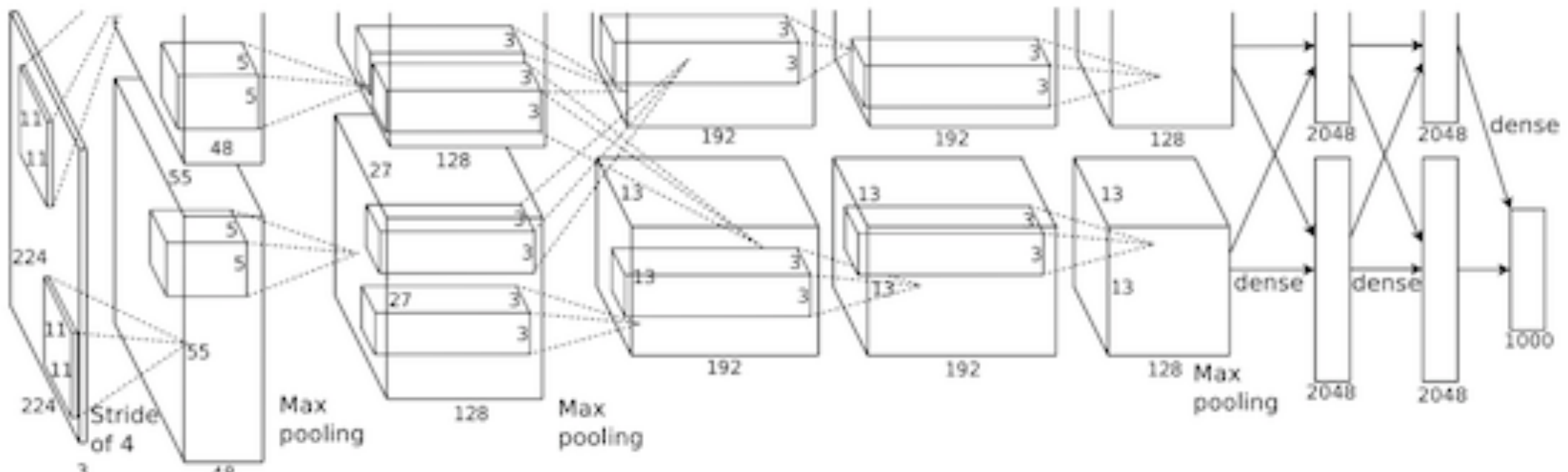


Sparse AE (SAE)



# Object Recognition

# Alex Net



## Innovations:

- Go Deep
- Train on Multiple GPUs
- ReLU
- DropOut
- Data Augmentation
- Response Normalization

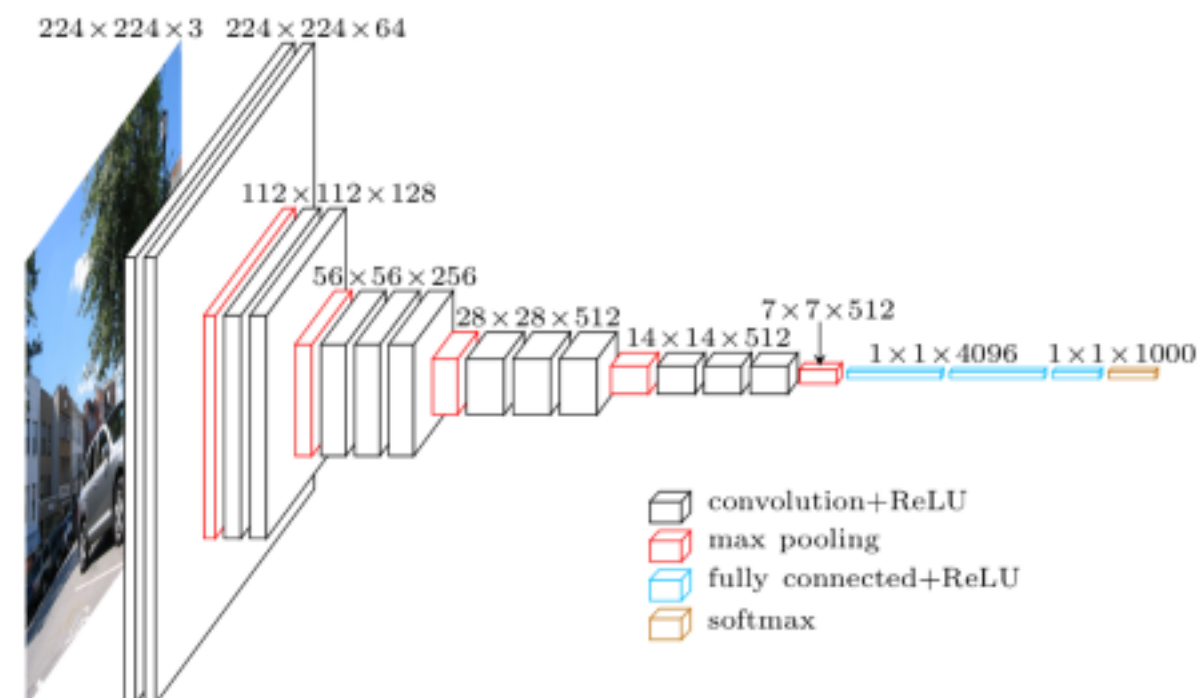


# VGG Net

why more convolutional layers?  
 1. same parameters, deeper network, more information;  
 2. parallel

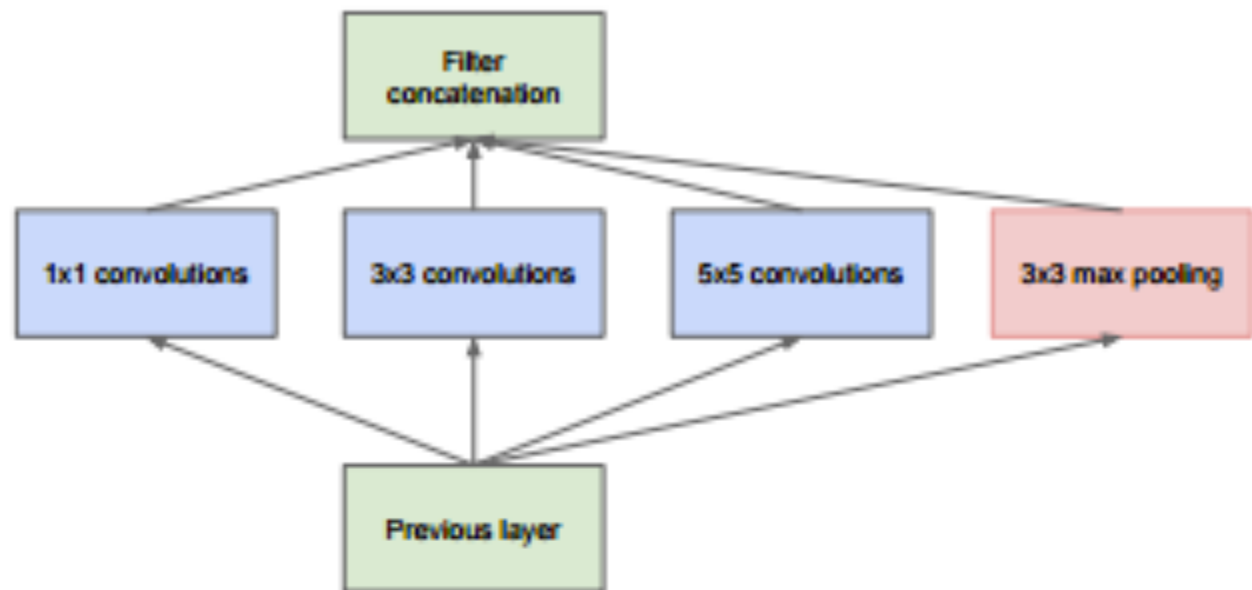
**Table 1: ConvNet configurations** (shown in columns). The depth of the configurations increases from the left (A) to the right (E), as more layers are added (the added layers are shown in bold). The convolutional layer parameters are denoted as “conv(receptive field size)-(number of channels)”. The ReLU activation function is not shown for brevity.

ConvNet Configuration					
A	A-LRN	B	C	D	E
11 weight layers	11 weight layers	13 weight layers	16 weight layers	16 weight layers	19 weight layers
input (224 × 224 RGB image)					
conv3-64	conv3-64 LRN	conv3-64	conv3-64	conv3-64	conv3-64
maxpool					
conv3-128	conv3-128	conv3-128	conv3-128	conv3-128	conv3-128
maxpool					
conv3-256	conv3-256	conv3-256	conv3-256	conv3-256	conv3-256
conv3-256	conv3-256	conv3-256	conv3-256	conv1-256	conv3-256
maxpool					
conv3-512	conv3-512	conv3-512	conv3-512	conv3-512	conv3-512
conv3-512	conv3-512	conv3-512	conv3-512	conv1-512	conv3-512
maxpool					
conv3-512	conv3-512	conv3-512	conv3-512	conv3-512	conv3-512
conv3-512	conv3-512	conv3-512	conv3-512	conv1-512	conv3-512
maxpool					
FC-4096					
FC-4096					
FC-1000					
soft-max					

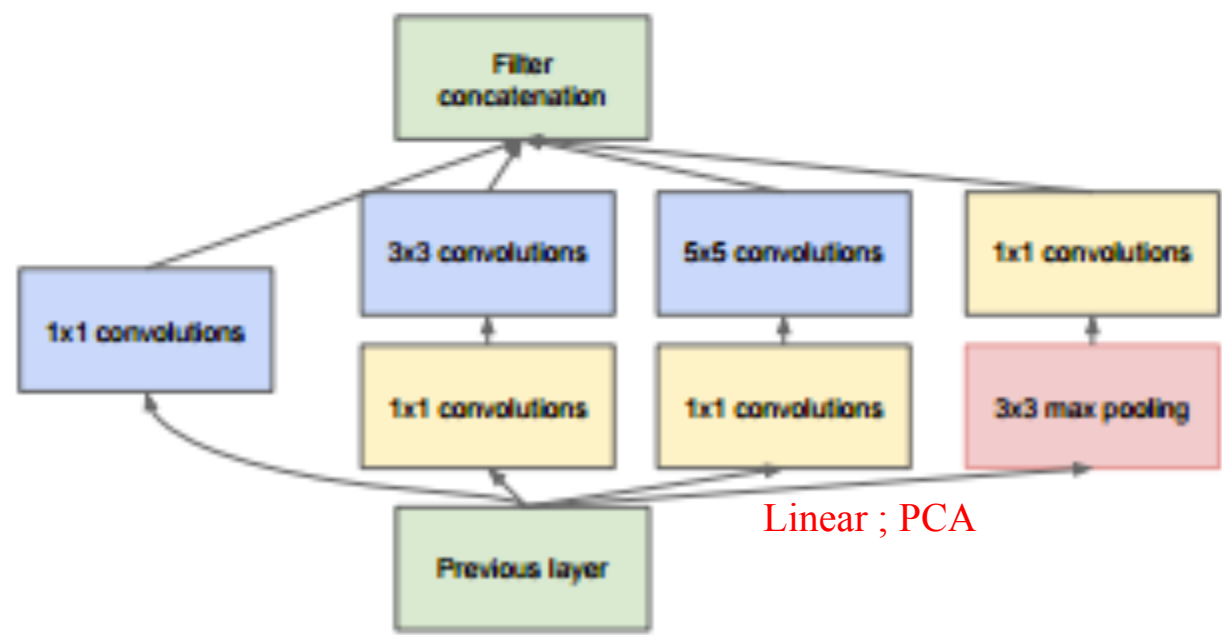


- ## Innovations:
- Replace one big filters by multiple smaller filters
  - Growing NNs

# GoogLeNet



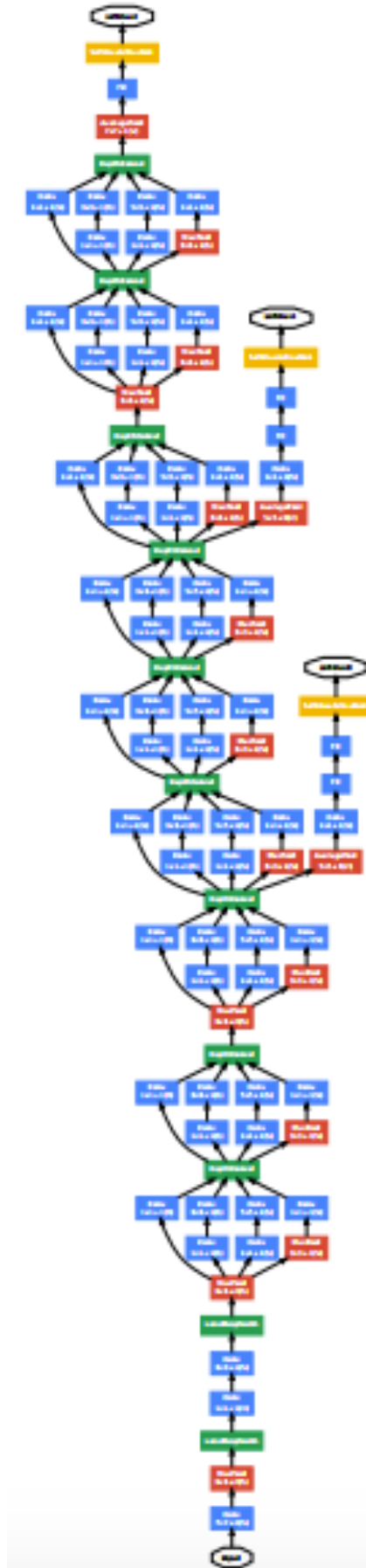
(a) Inception module, naïve version



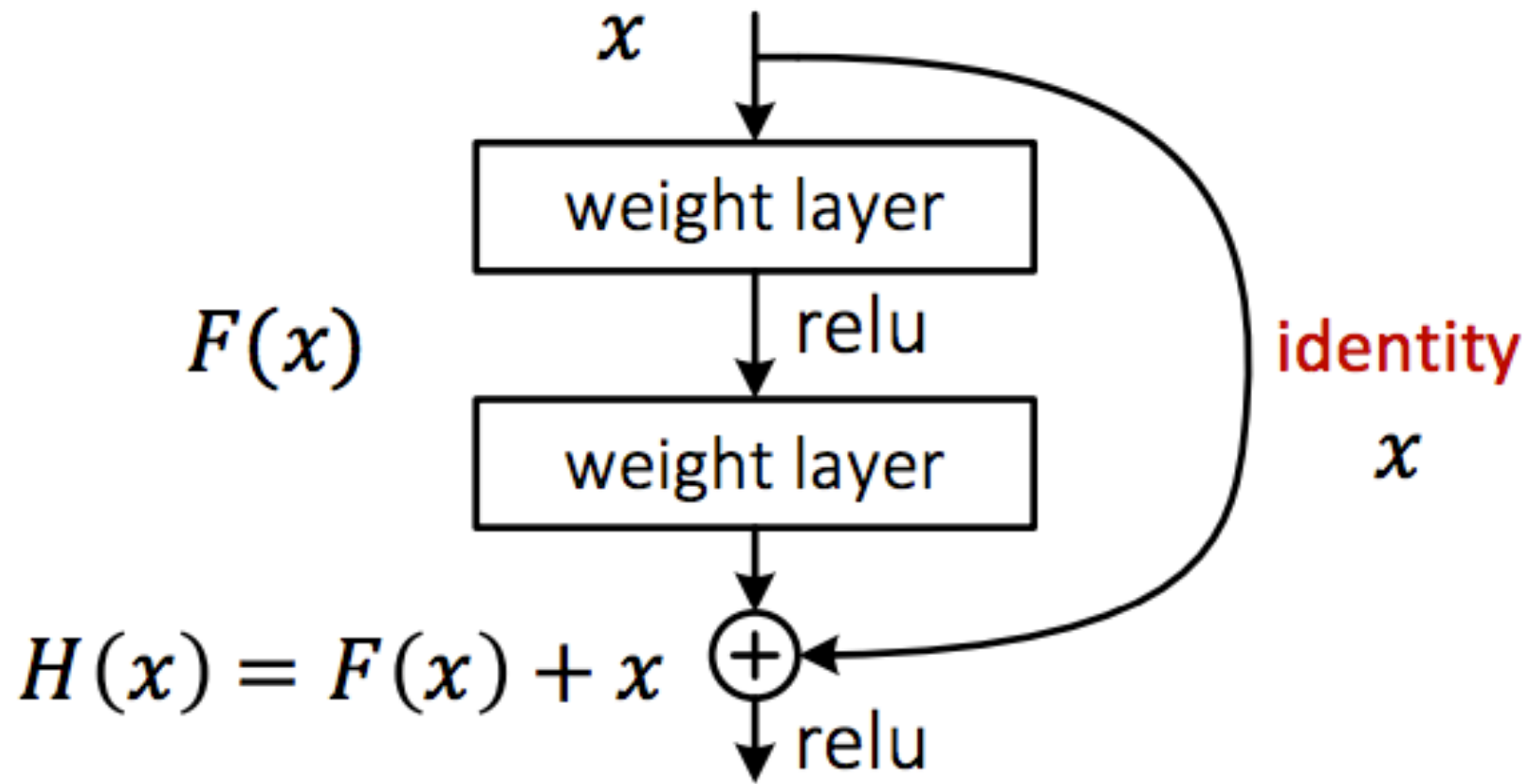
(b) Inception module with dimensionality reduction

## Innovations:

- Scale-Pooling
- 1x1 Conv (Dim. Reduction)



# ResNet



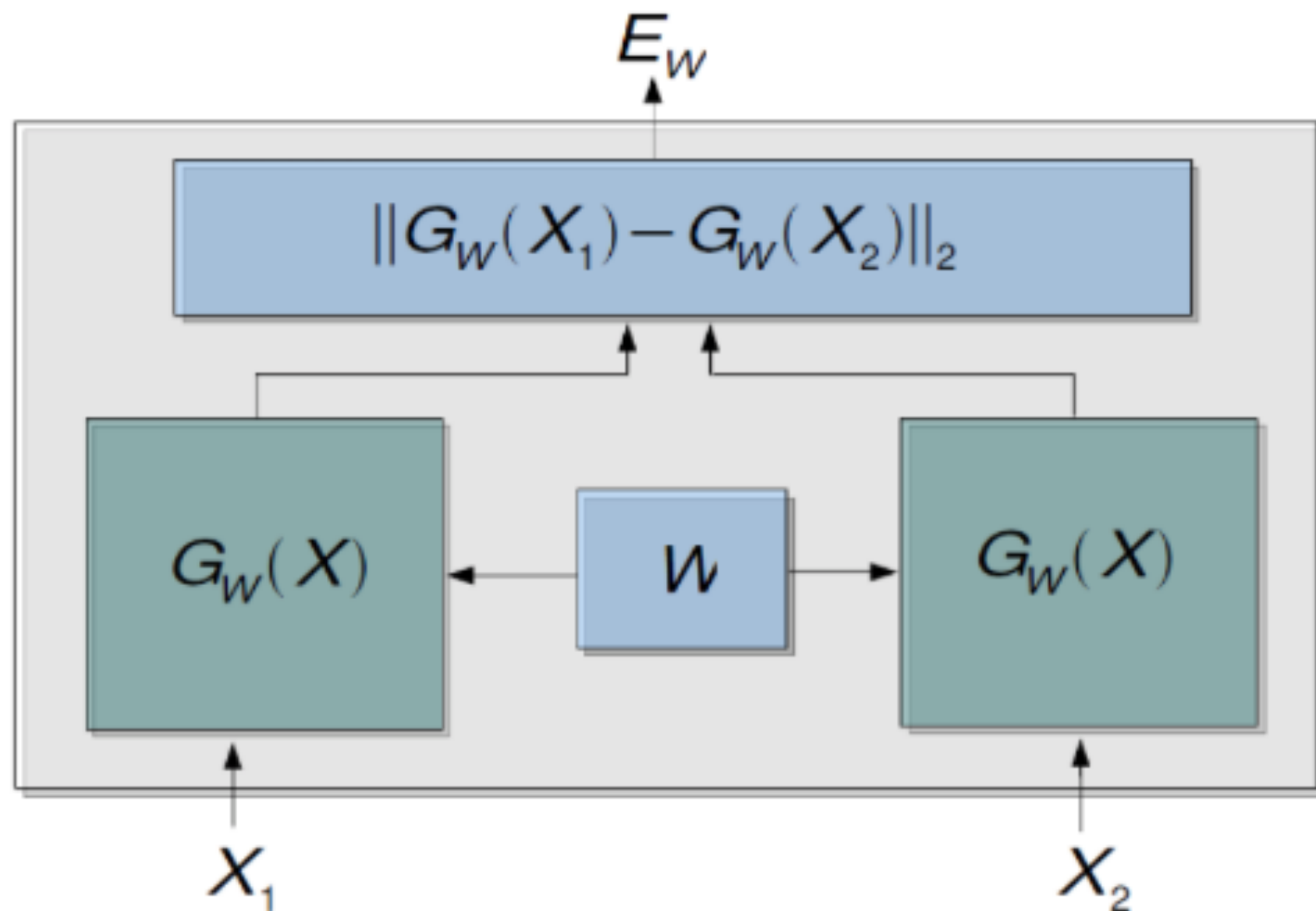
## Innovation:

- Make it easy to express identity
- Preconditioning

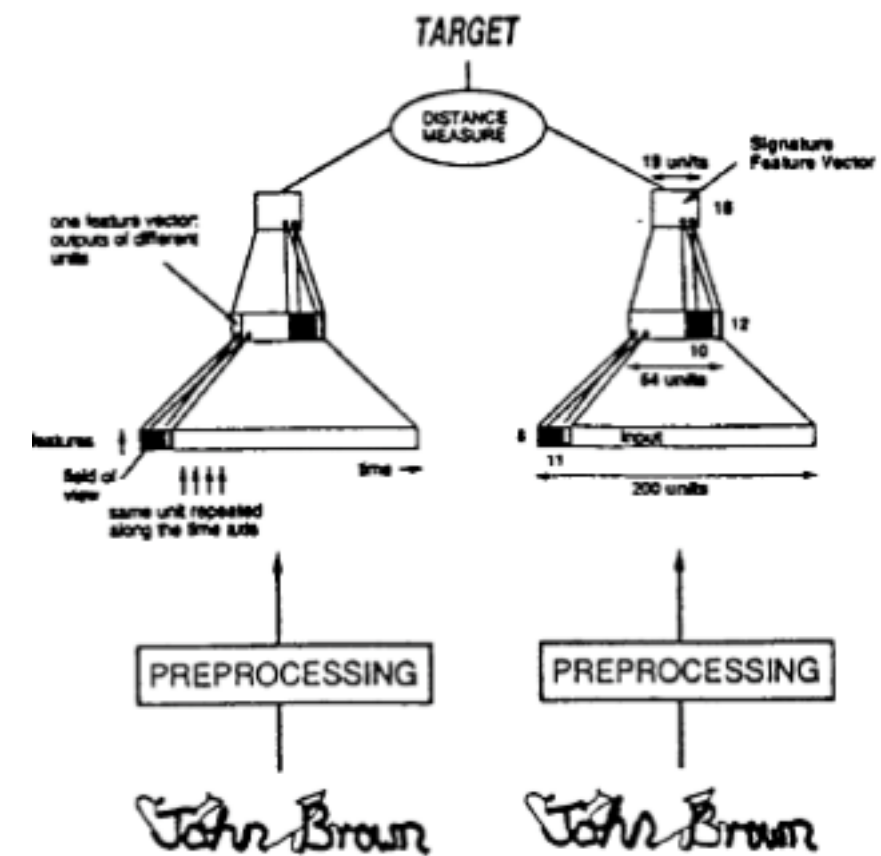
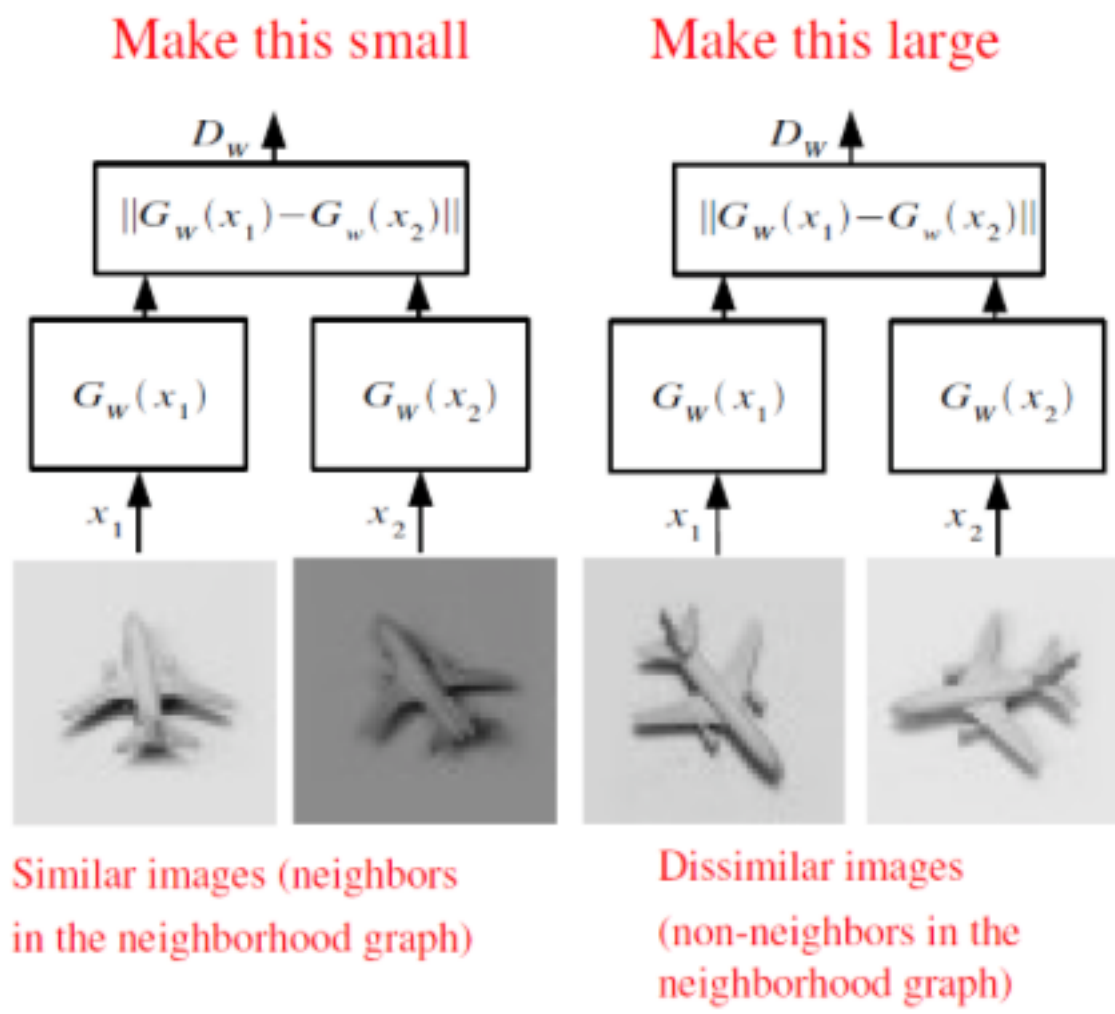


# Siamese Networks

# Siamese Networks for Similarity Discrimination/Matching



# Siamese Networks for Similarity Discrimination/Matching



*Learning Hierarchies of Invariant Features.* Yann LeCun.  
[helper.ipam.ucla.edu/publications/gss2012/gss2012\\_10739.pdf](http://helper.ipam.ucla.edu/publications/gss2012/gss2012_10739.pdf)

Bromley J, Guyon I, LeCun Y, et al. *Signature Verification using a "Siamese" Time Delay Neural Network*, NIPS Proc. 1994.

# Face Recognition

# DeepFace

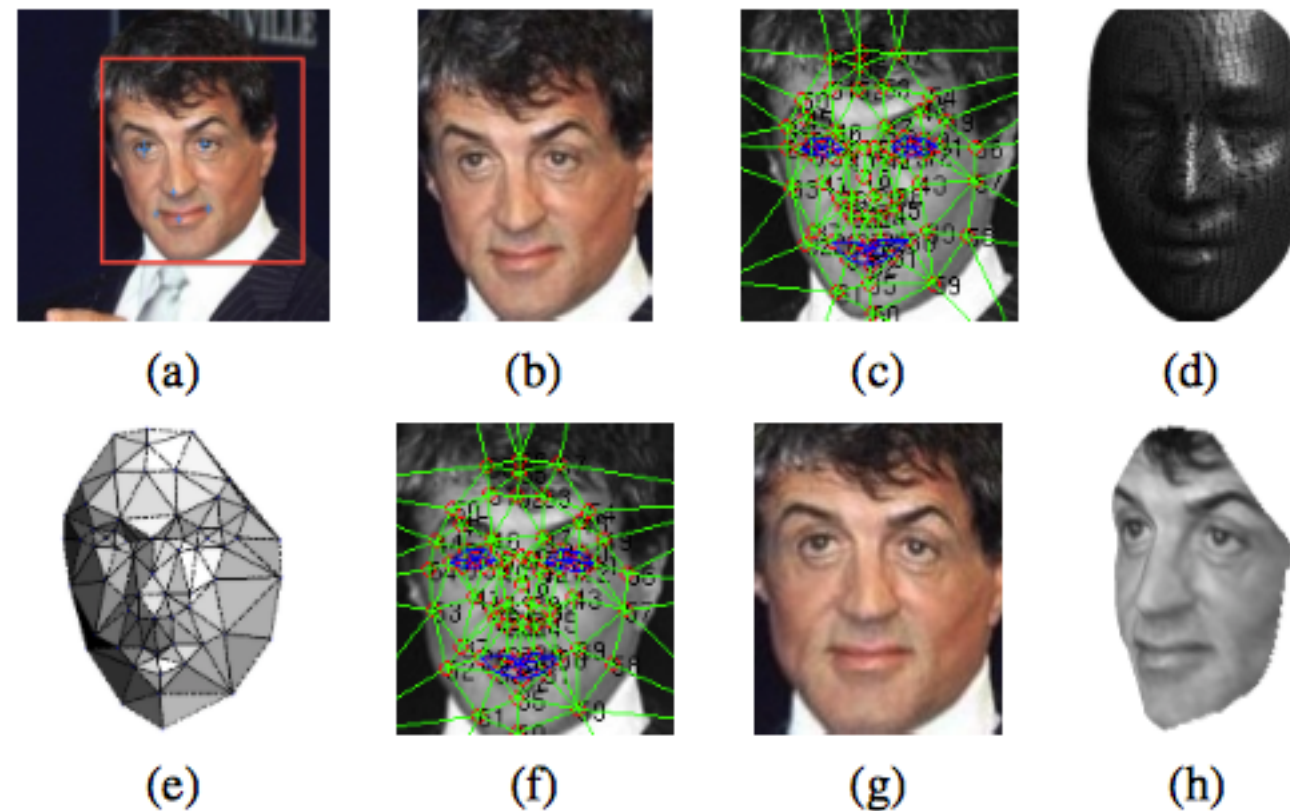


**Figure 1. Alignment pipeline.** (a) The detected face, with 6 initial fiducial points. (b) The induced 2D-aligned crop. (c) 67 fiducial points on the 2D-aligned crop with their corresponding Delaunay triangulation, we added triangles on the contour to avoid discontinuities. (d) The reference 3D shape transformed to the 2D-aligned crop image-plane. (e) Triangle visibility w.r.t. to the fitted 3D-2D camera; darker triangles are less visible. (f) The 67 fiducial points induced by the 3D model that are used to direct the piece-wise affine warpping. (g) The final frontalized crop. (h) A new view generated by the 3D model (not used in this paper).

# DeepFace

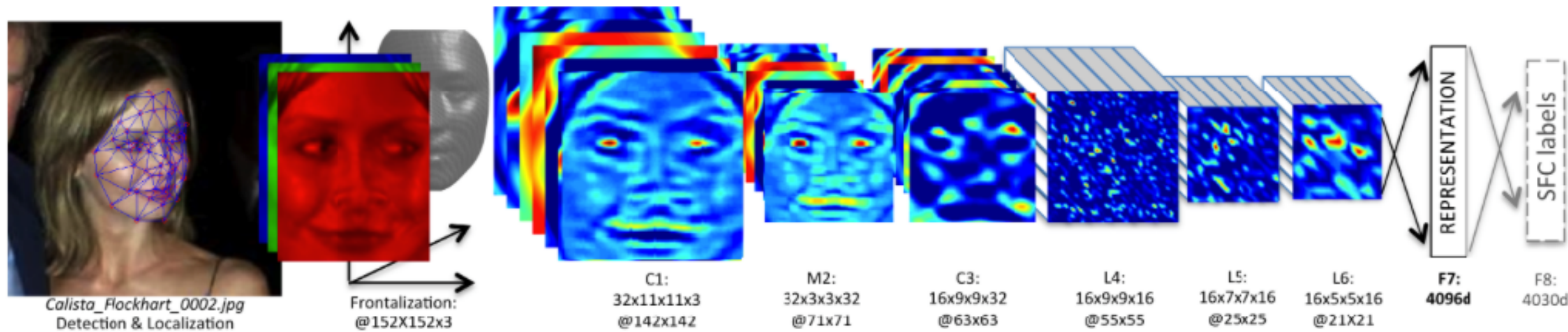


**Figure 2. Outline of the *DeepFace* architecture.** A front-end of a single convolution-pooling-convolution filtering on the rectified input, followed by three locally-connected layers and two fully-connected layers. Colors illustrate feature maps produced at each layer. The net includes more than 120 million parameters, where more than 95% come from the local and fully connected layers.

# DeepFace

Method	Accuracy $\pm$ SE	Protocol
Joint Bayesian [6]	$0.9242 \pm 0.0108$	restricted
Tom-vs-Pete [4]	$0.9330 \pm 0.0128$	restricted
High-dim LBP [7]	$0.9517 \pm 0.0113$	restricted
TL Joint Bayesian [5]	$0.9633 \pm 0.0108$	restricted
DeepFace-single	<b><math>0.9592 \pm 0.0029</math></b>	unsupervised
DeepFace-single	<b><math>0.9700 \pm 0.0028</math></b>	restricted
DeepFace-ensemble	<b><math>0.9715 \pm 0.0027</math></b>	restricted
DeepFace-ensemble	<b><math>0.9735 \pm 0.0025</math></b>	unrestricted
Human, cropped	0.9753	

Table 3. Comparison with the state-of-the-art on the *LFW* dataset.

Method	Accuracy (%)	AUC	EER
MBGS+SVM- [31]	$78.9 \pm 1.9$	86.9	21.2
APEM+FUSION [22]	$79.1 \pm 1.5$	86.6	21.4
STFRD+PMML [9]	$79.5 \pm 2.5$	88.6	19.9
VSOF+OSS [23]	$79.7 \pm 1.8$	89.4	20.0
DeepFace-single	<b><math>91.4 \pm 1.1</math></b>	96.3	8.6

Table 4. Comparison with the state-of-the-art on the *YTF* dataset.

# FaceNet



Figure 2. **Model structure.** Our network consists of a batch input layer and a deep CNN followed by  $L_2$  normalization, which results in the face embedding. This is followed by the triplet loss during training.

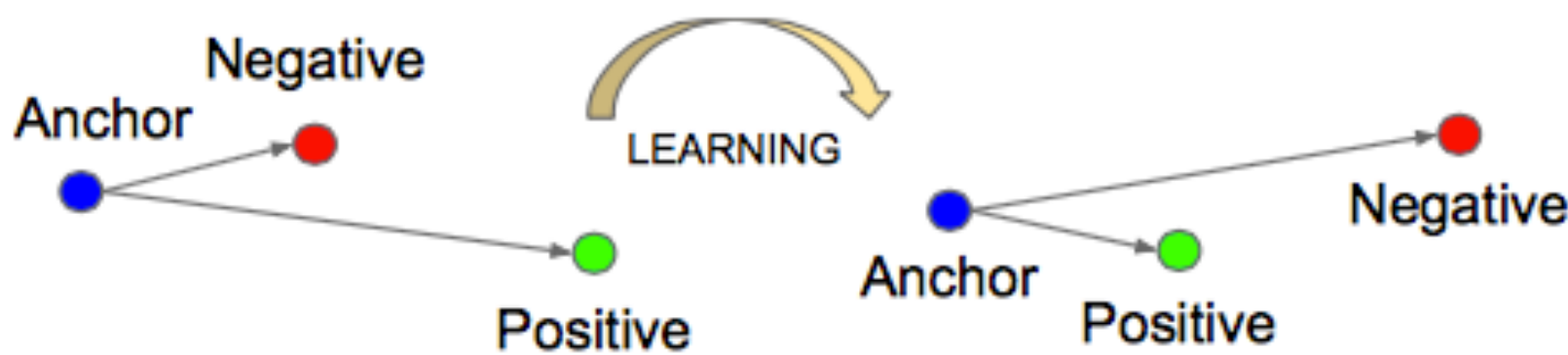


Figure 3. The **Triplet Loss** minimizes the distance between an *anchor* and a *positive*, both of which have the same identity, and maximizes the distance between the *anchor* and a *negative* of a different identity.

# FaceNet

- Labeled Faces in the Wild:  
No alignment: 98.87%  
 $\pm 0.15$   
With alignment: 99.63%  
 $\pm 0.09$
- Youtube Faces DB:  
95.12%  $\pm 0.39$  (state-of-the-art)

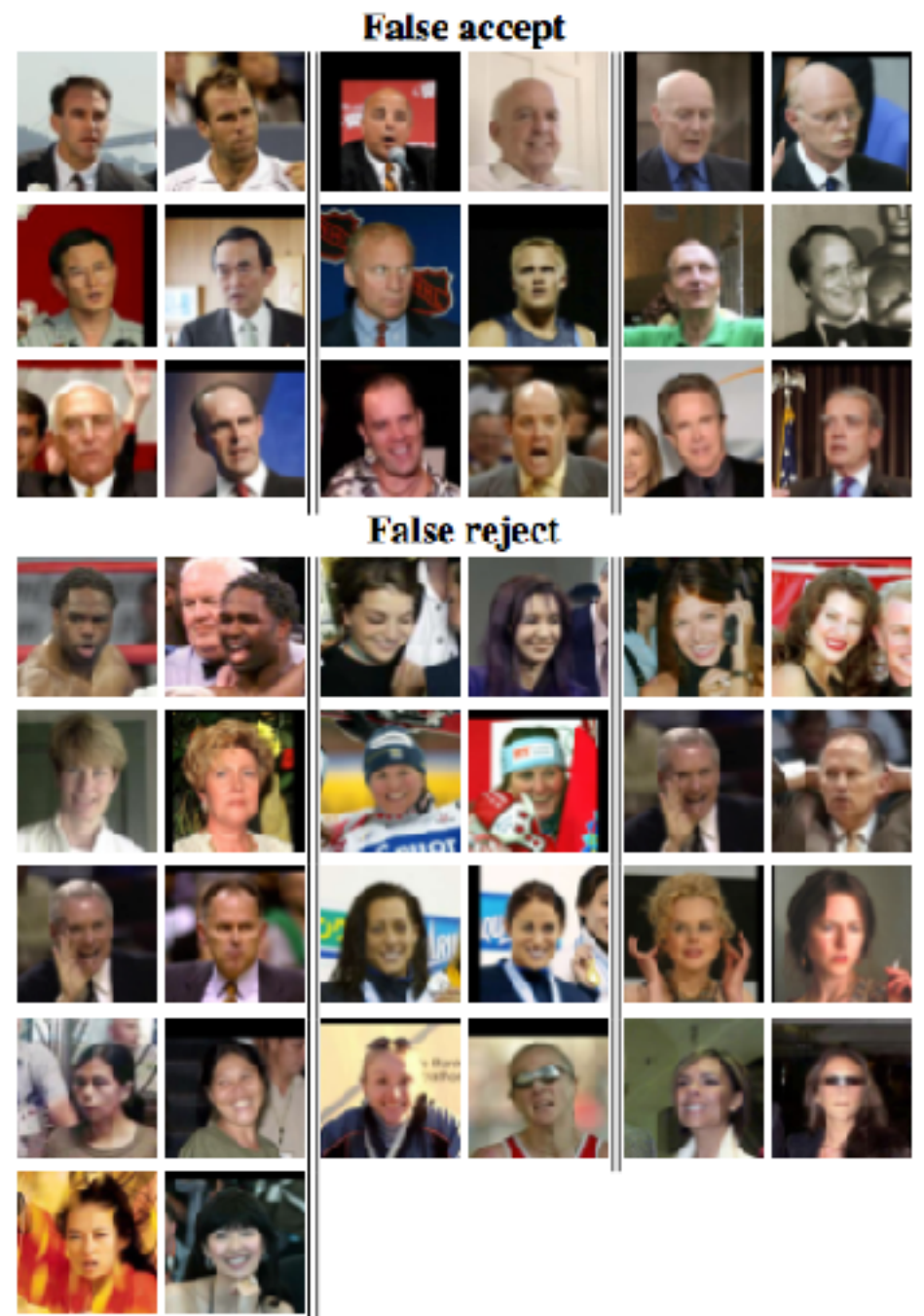


Figure 6. **LFW errors.** This shows all pairs of images that were incorrectly classified on LFW. Only eight of the 13 false rejects shown here are actual errors the other five are mislabeled in LFW.

# Object Tracking

# Visual Examples



# MDNet: Convnet for Object Tracking

**MDNet (Multi-Domain Network)**

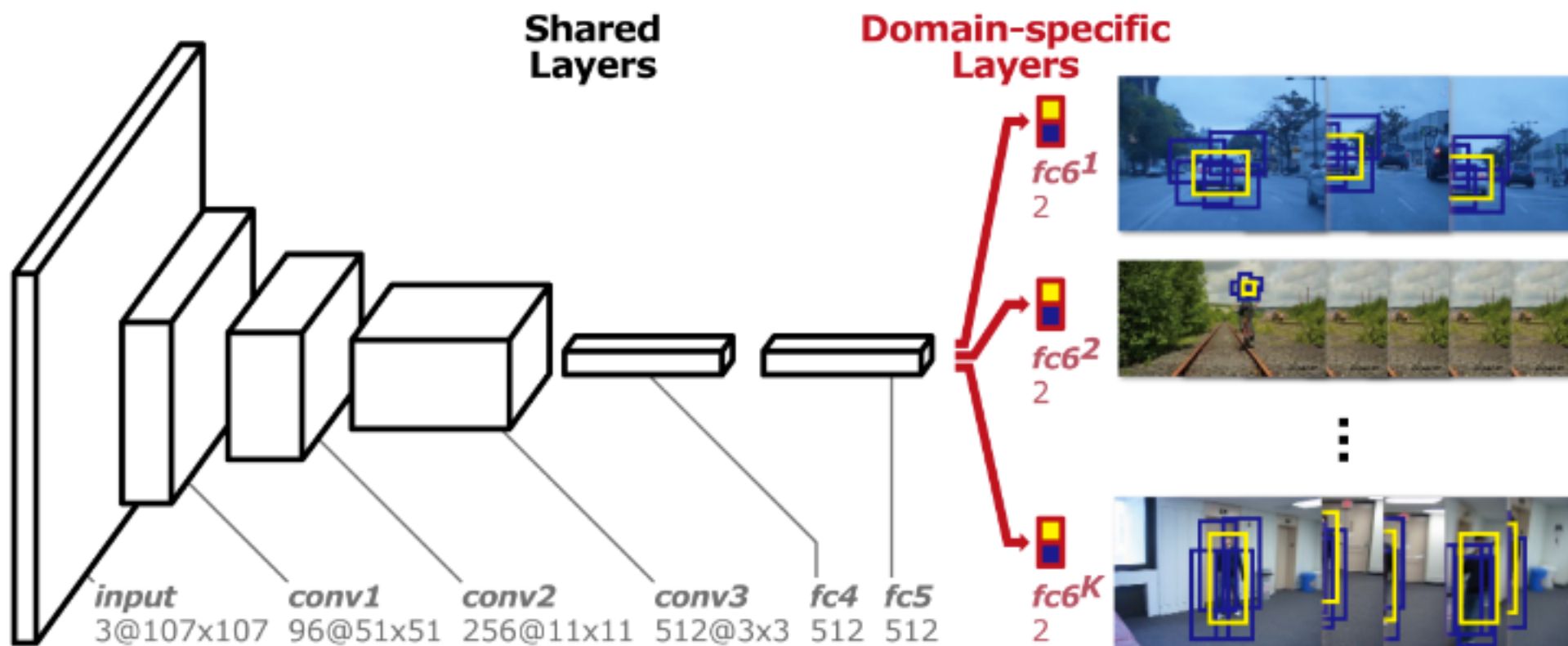
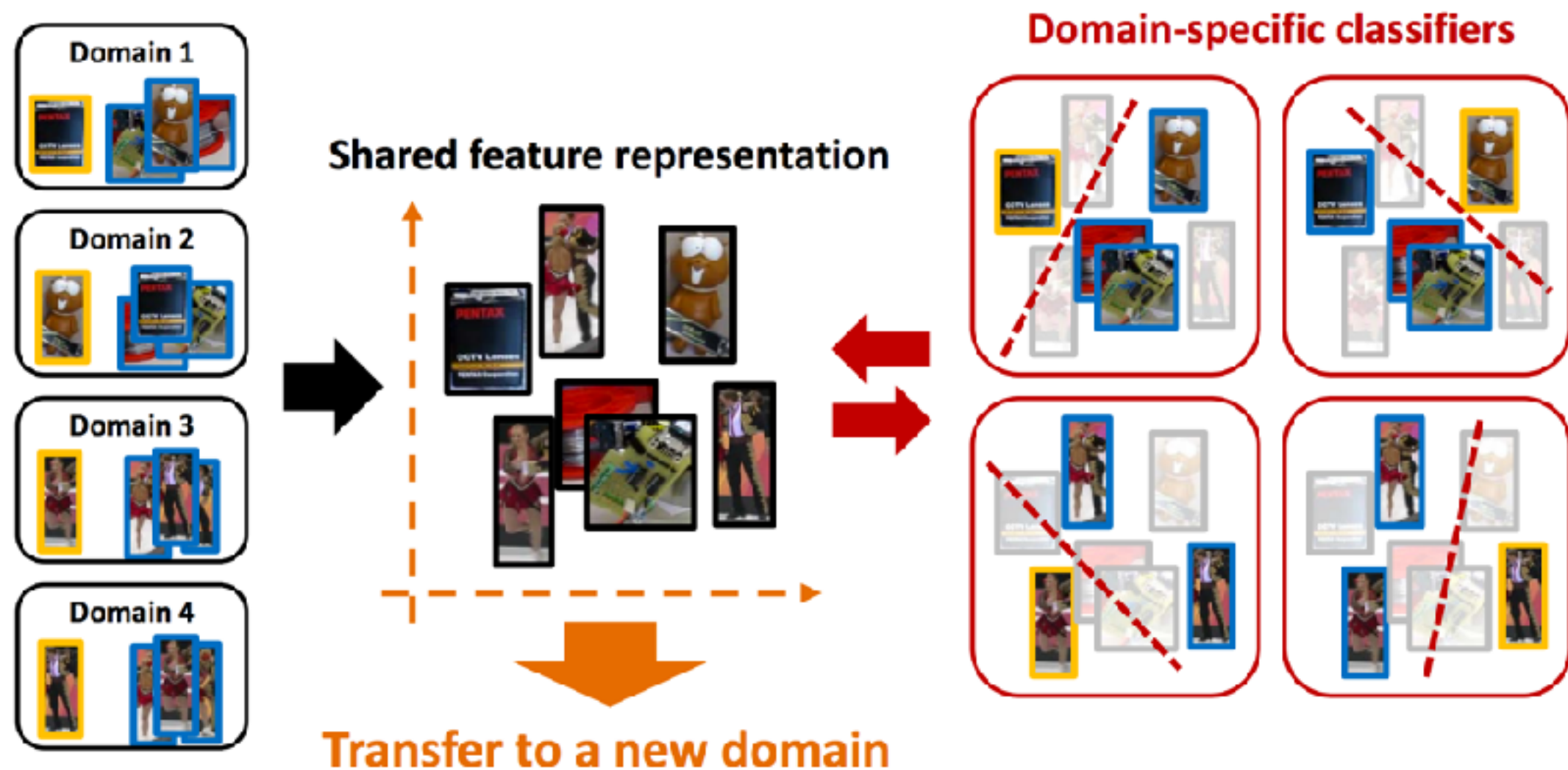
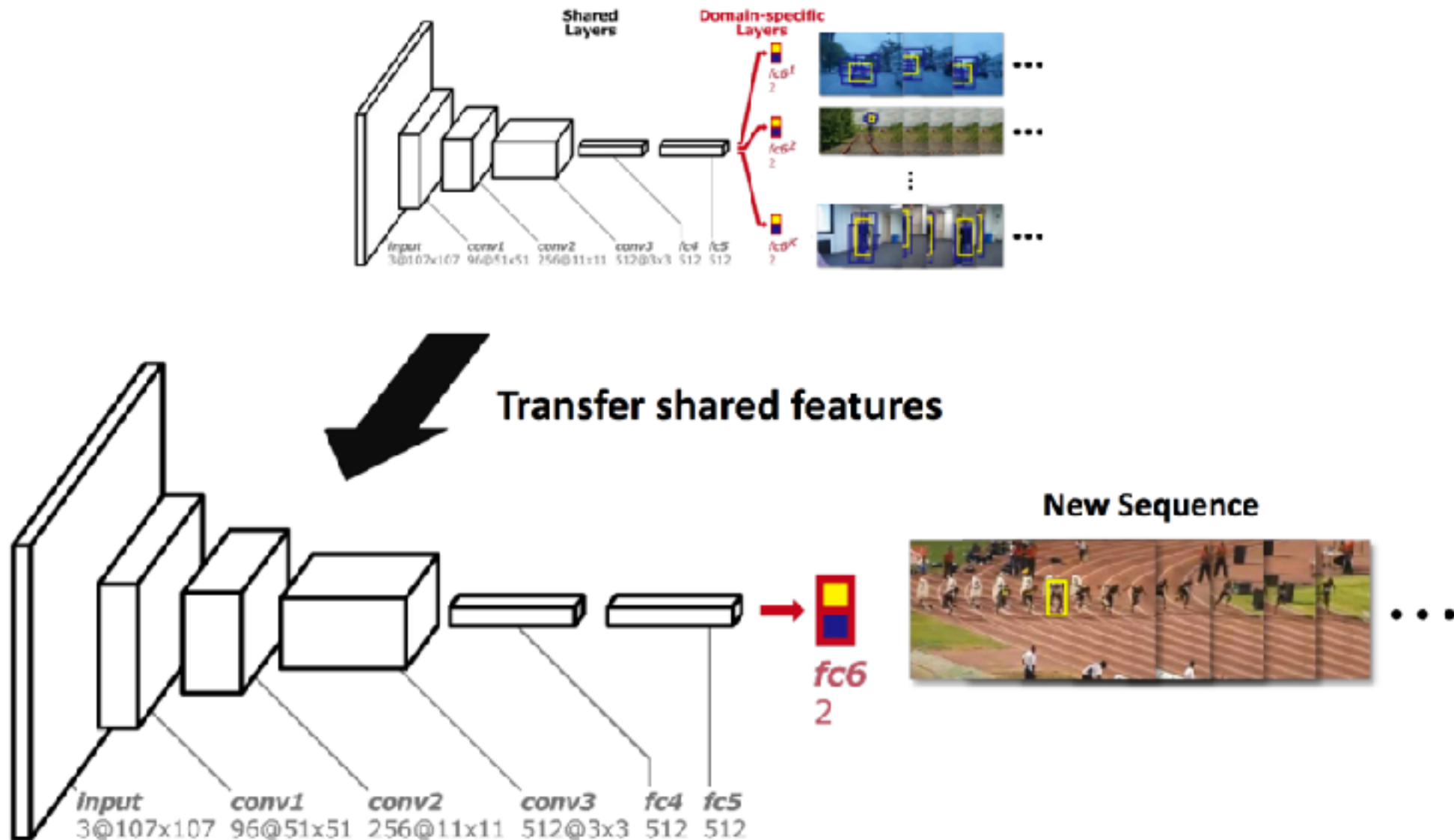


**Figure 1.** The architecture of our Multi-Domain Network (MDNet), which consists of shared layers and multiple branches of domain-specific layers. Yellow and blue bounding boxes denote the positive and negative training samples in each domain, respectively.

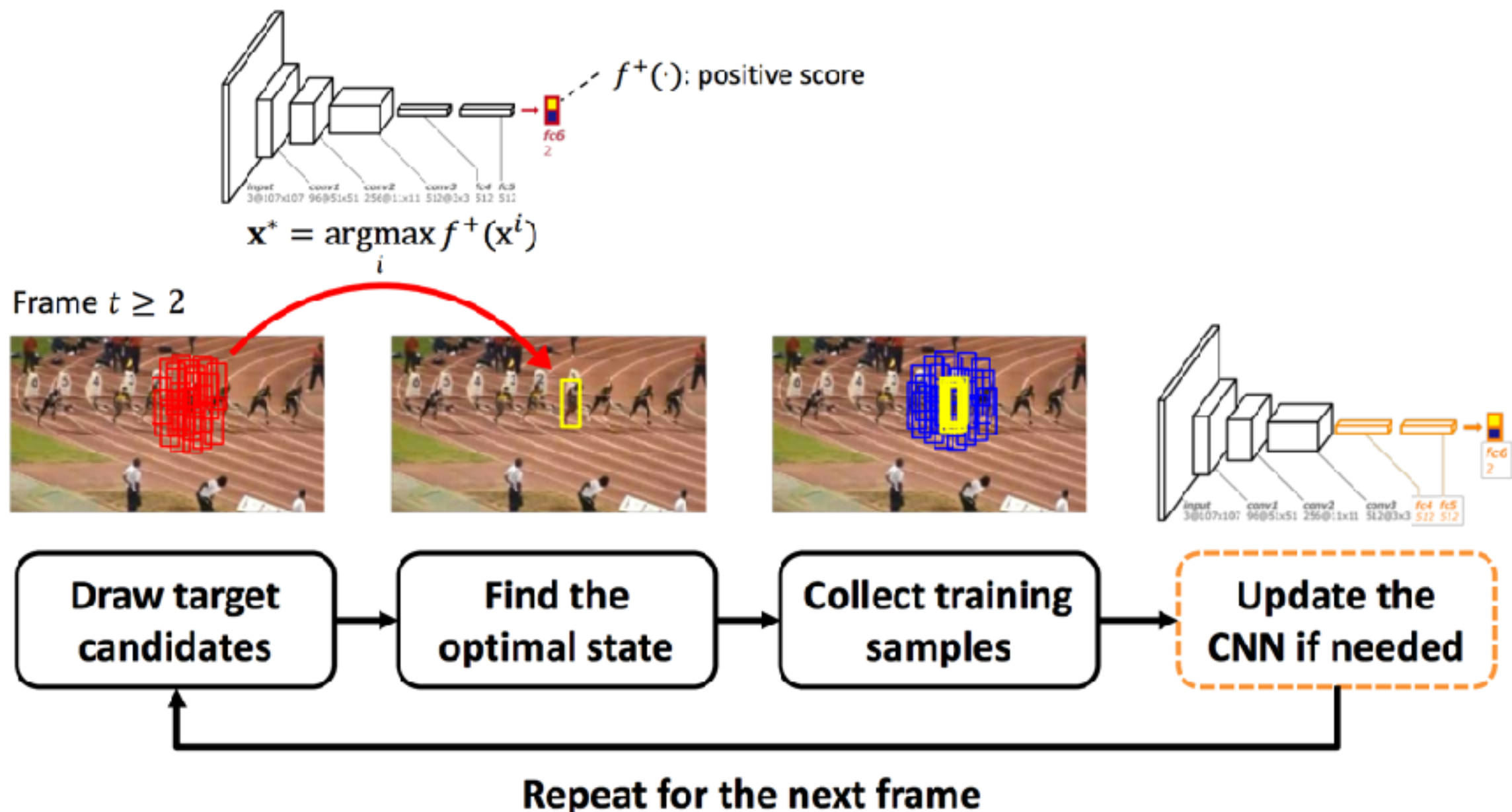
# Which Object is the Target?



# Test Time: Transferring the Shared Features to Standard Convnet



# Test Time: Transferring the Shared Features to Standard Convnet



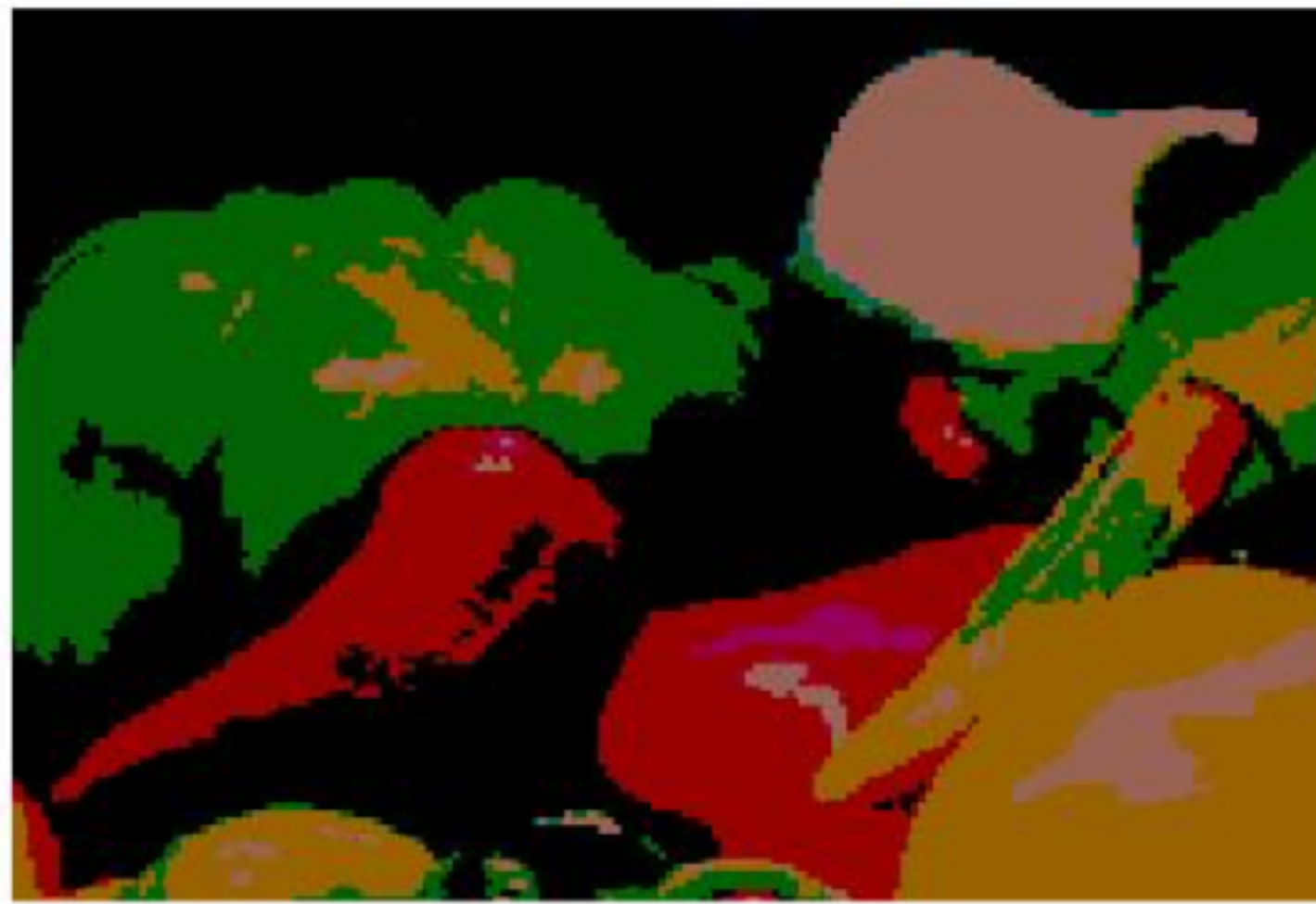
# MDNet Video Results

Learning Multi-Domain Convolutional  
Neural Networks for Visual Tracking

Hyeonseob Nam and Bohyung Han

# Image Segmentation

# Image Segmentation



# Fully Convolutional Networks for Semantic Segmentation

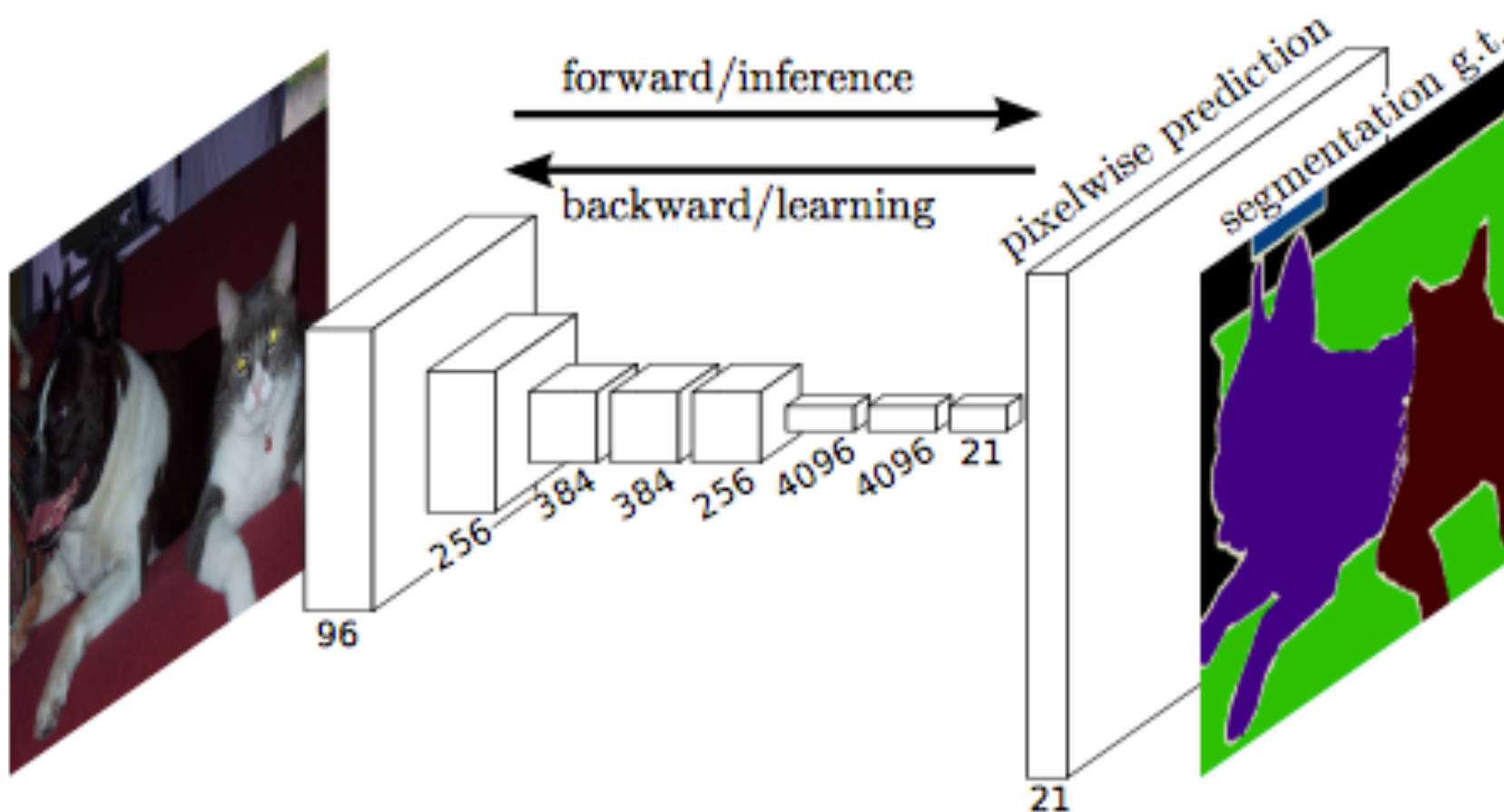


Figure 1. Fully convolutional networks can efficiently learn to make dense predictions for per-pixel tasks like semantic segmentation.

[Jonathan Long, Evan Shelhamer, Yann LeCun]

# Fully Convolutional Networks for Semantic Segmentation

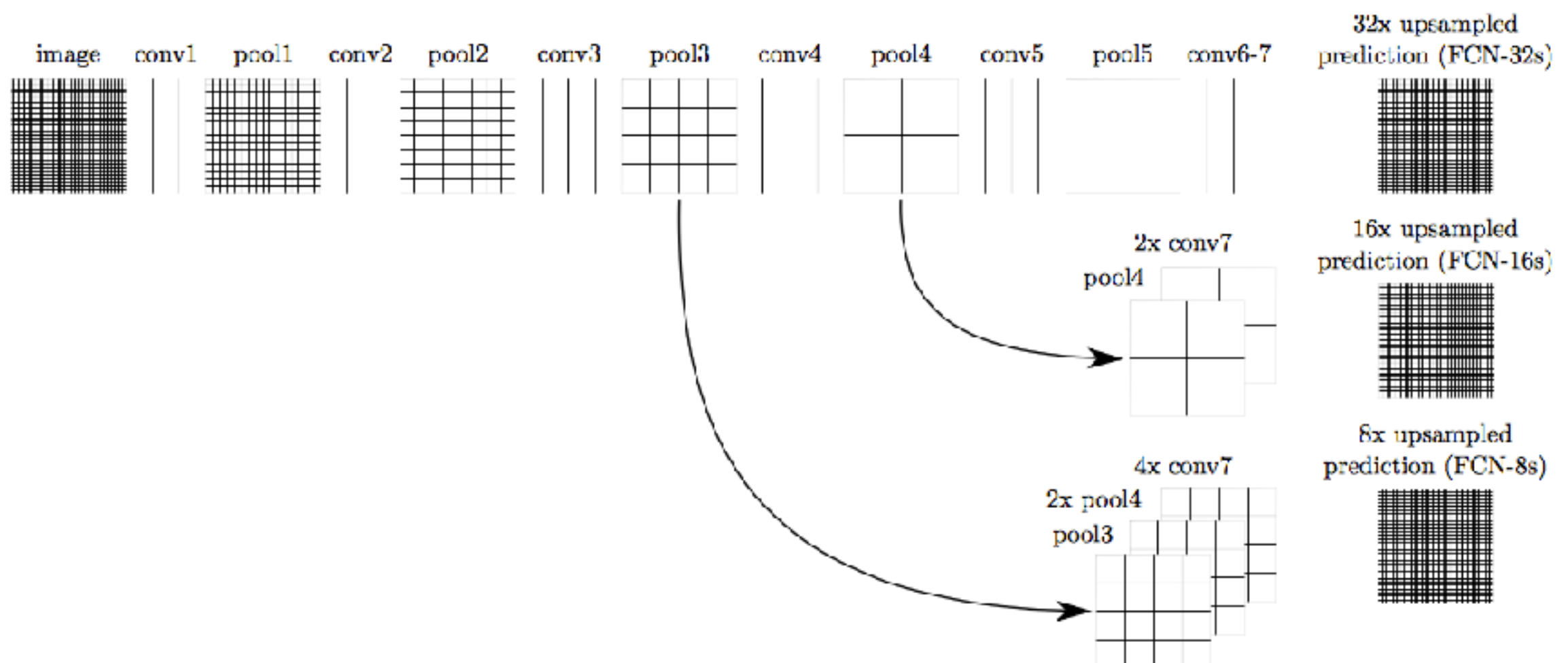


Figure 3. Our DAG nets learn to combine coarse, high layer information with fine, low layer information. Pooling and prediction layers are shown as grids that reveal relative spatial coarseness, while intermediate layers are shown as vertical lines. First row (FCN-32s): Our single-stream net, described in Section 4.1, upsamples stride 32 predictions back to pixels in a single step. Second row (FCN-16s): Combining predictions from both the final layer and the pool4 layer, at stride 16, lets our net predict finer details, while retaining high-level semantic information. Third row (FCN-8s): Additional predictions from pool3, at stride 8, provide further precision.

[Jonathan Long, Evan Shelhamer, Yann LeCun]

# Fully Convolutional Networks for Semantic Segmentation

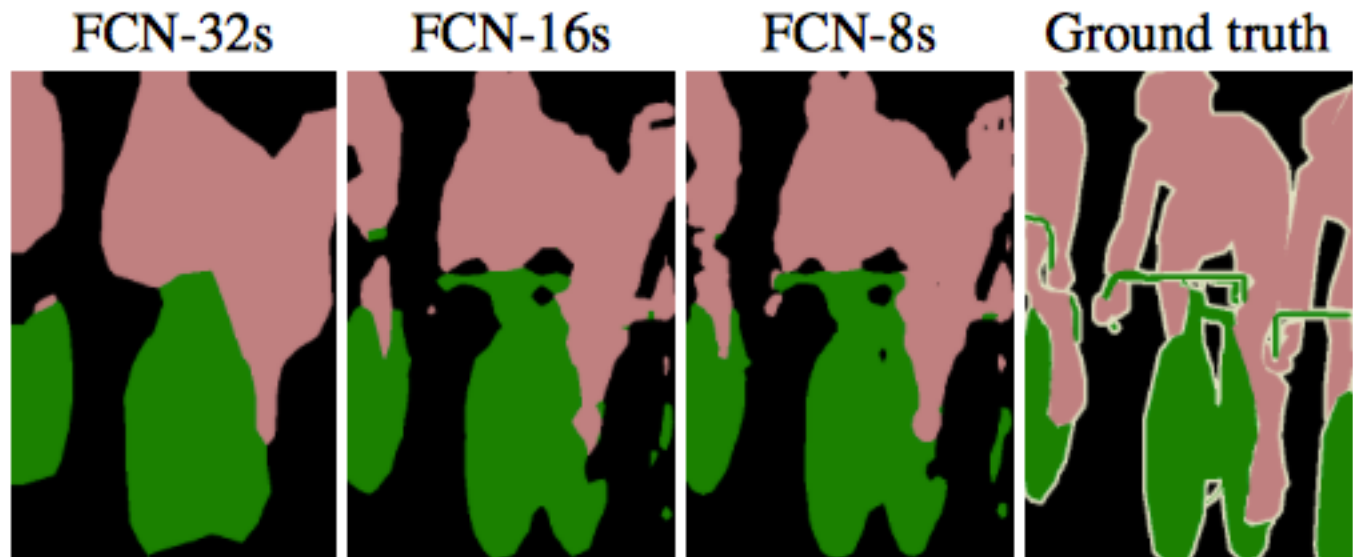


Figure 4. Refining fully convolutional nets by fusing information from layers with different strides improves segmentation detail. The first three images show the output from our 32, 16, and 8 pixel stride nets (see Figure 3).

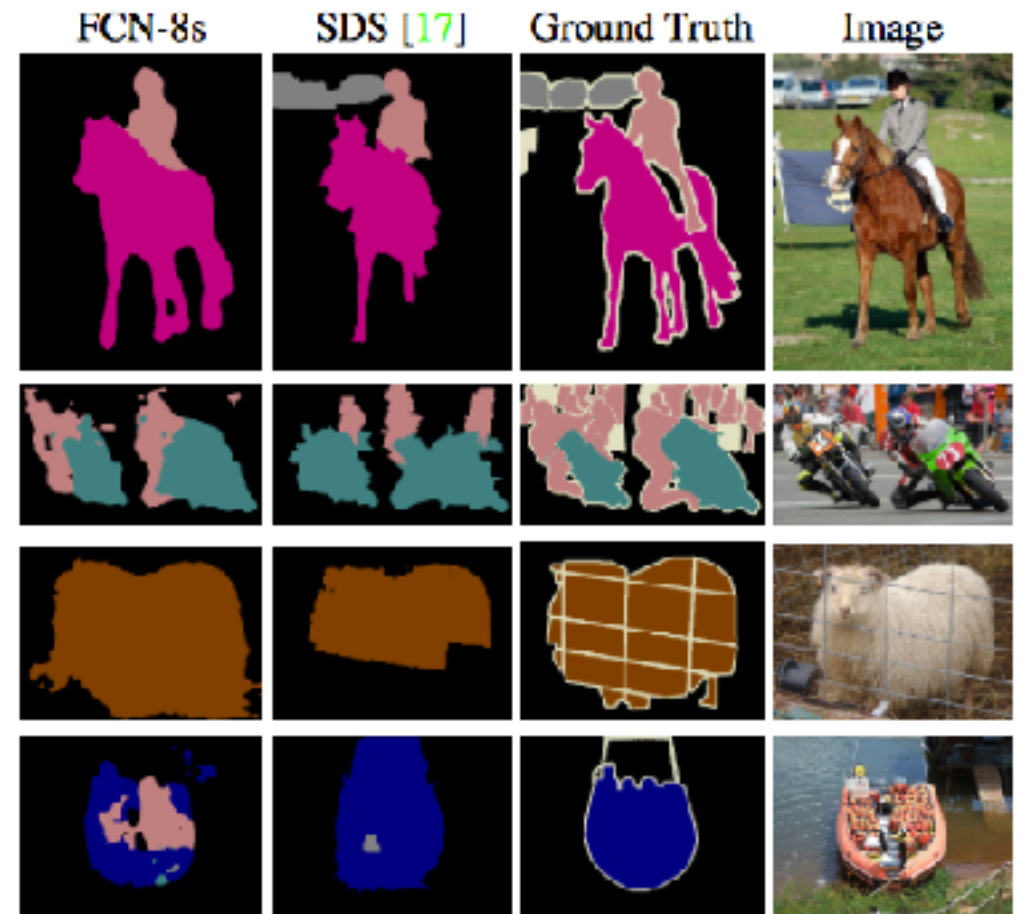


Figure 6. Fully convolutional segmentation nets produce state-of-the-art performance on PASCAL. The left column shows the output of our highest performing net, FCN-8s. The second shows the segmentations produced by the previous state-of-the-art system by Hariharan *et al.* [17]. Notice the fine structures recovered (first row), ability to separate closely interacting objects (second row), and robustness to occluders (third row). The fourth row shows a failure case: the net sees lifejackets in a boat as people.

[Jonathan Long, Evan Shelhamer, Yann LeCun]

# Stereo Matching

# Stereo Convnets

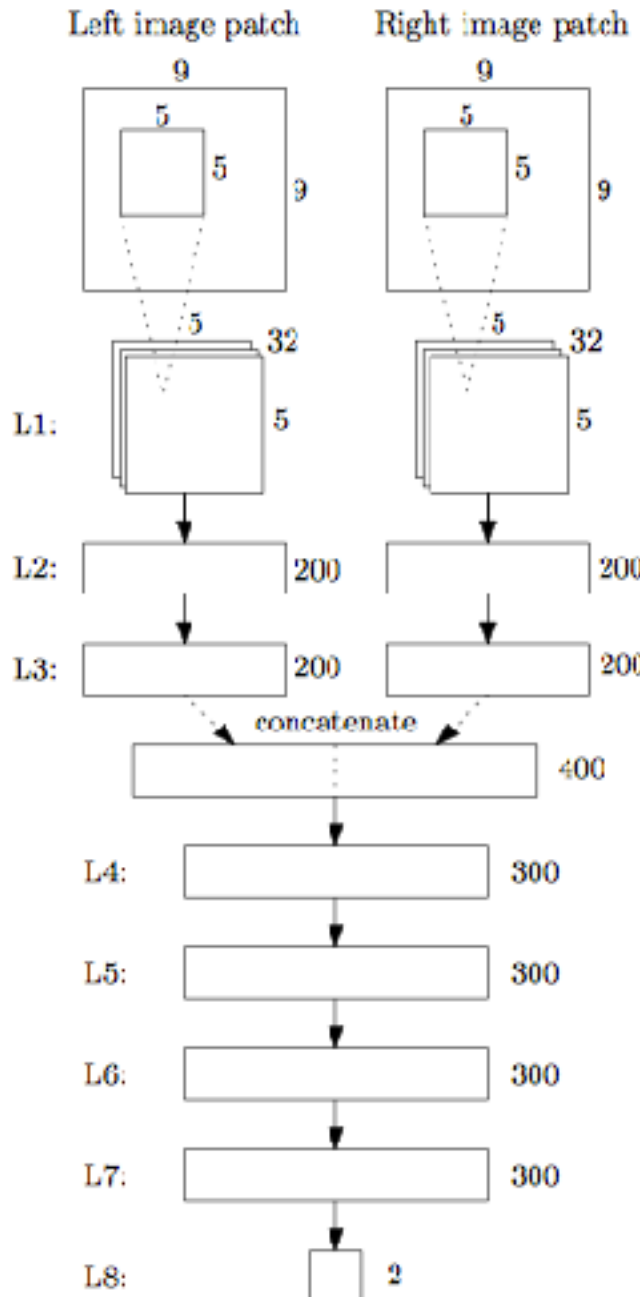


Figure 2. The architecture of our convolutional neural network.

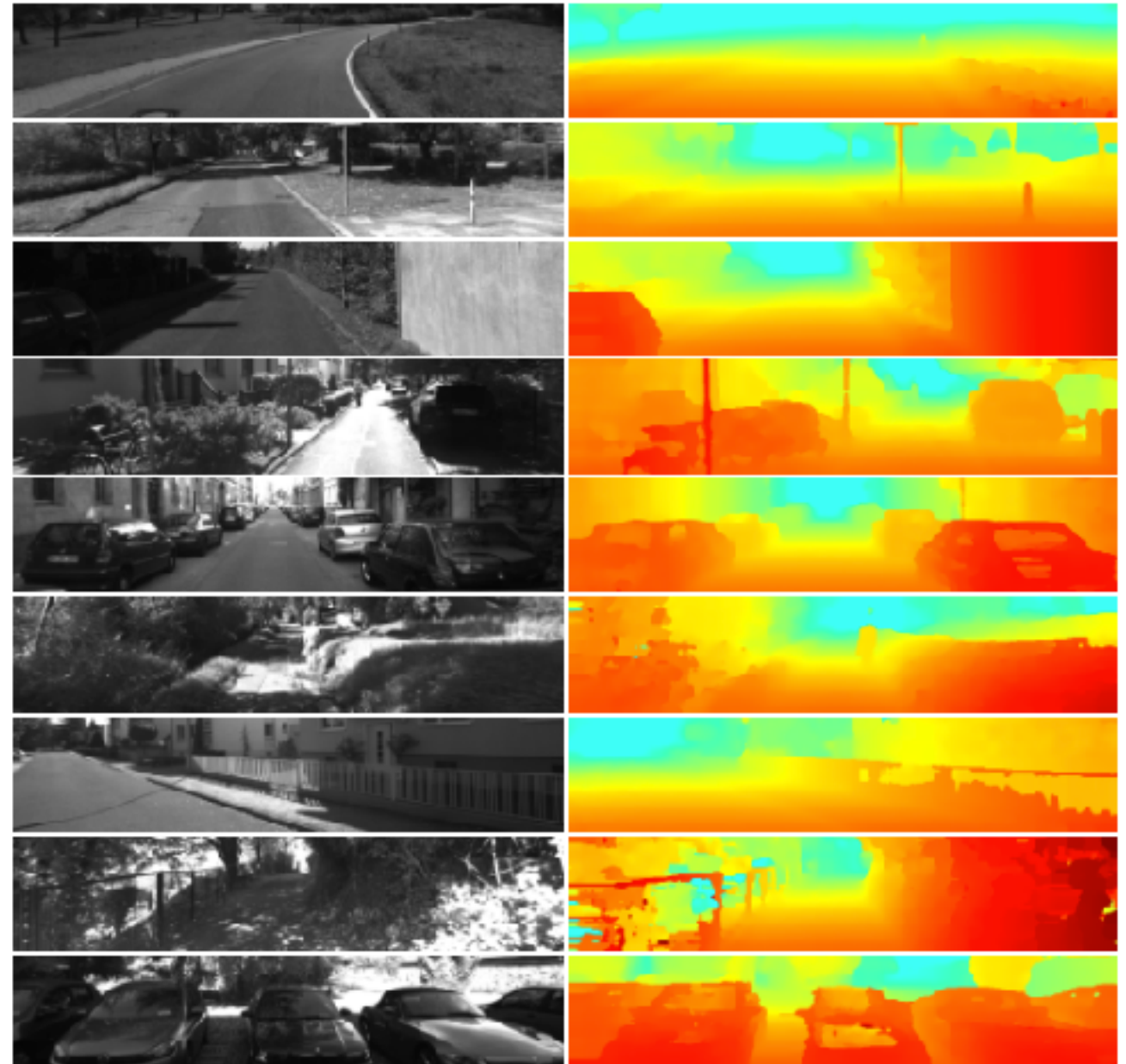


Figure 5. The left column displays the left input image, while the right column displays the output of our stereo method. Examples are sorted by difficulty, with easy examples appearing at the top. Some of the difficulties include reflective surfaces, occlusions, as well as regions with many jumps in disparity, e.g. fences and shrubbery. The examples towards the bottom were selected to highlight the flaws in our method and to demonstrate the inherent difficulties of stereo matching on real-world images.

[Jure Zbontar, Yann LeCun]

# Speech Synthesis

# WaveNet

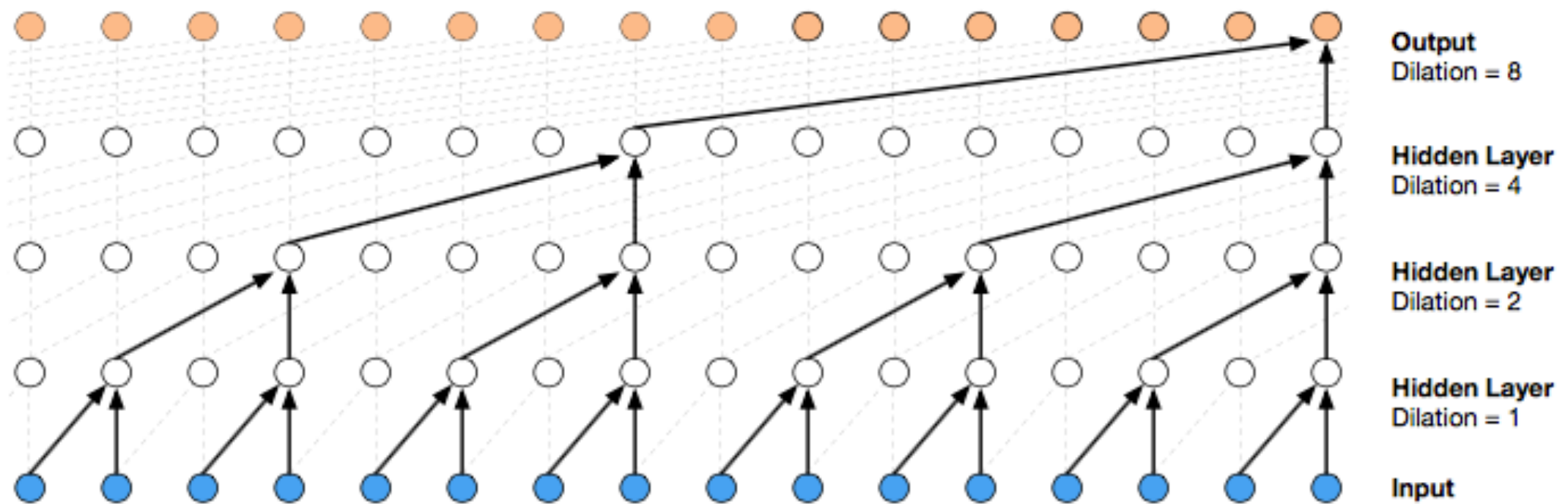
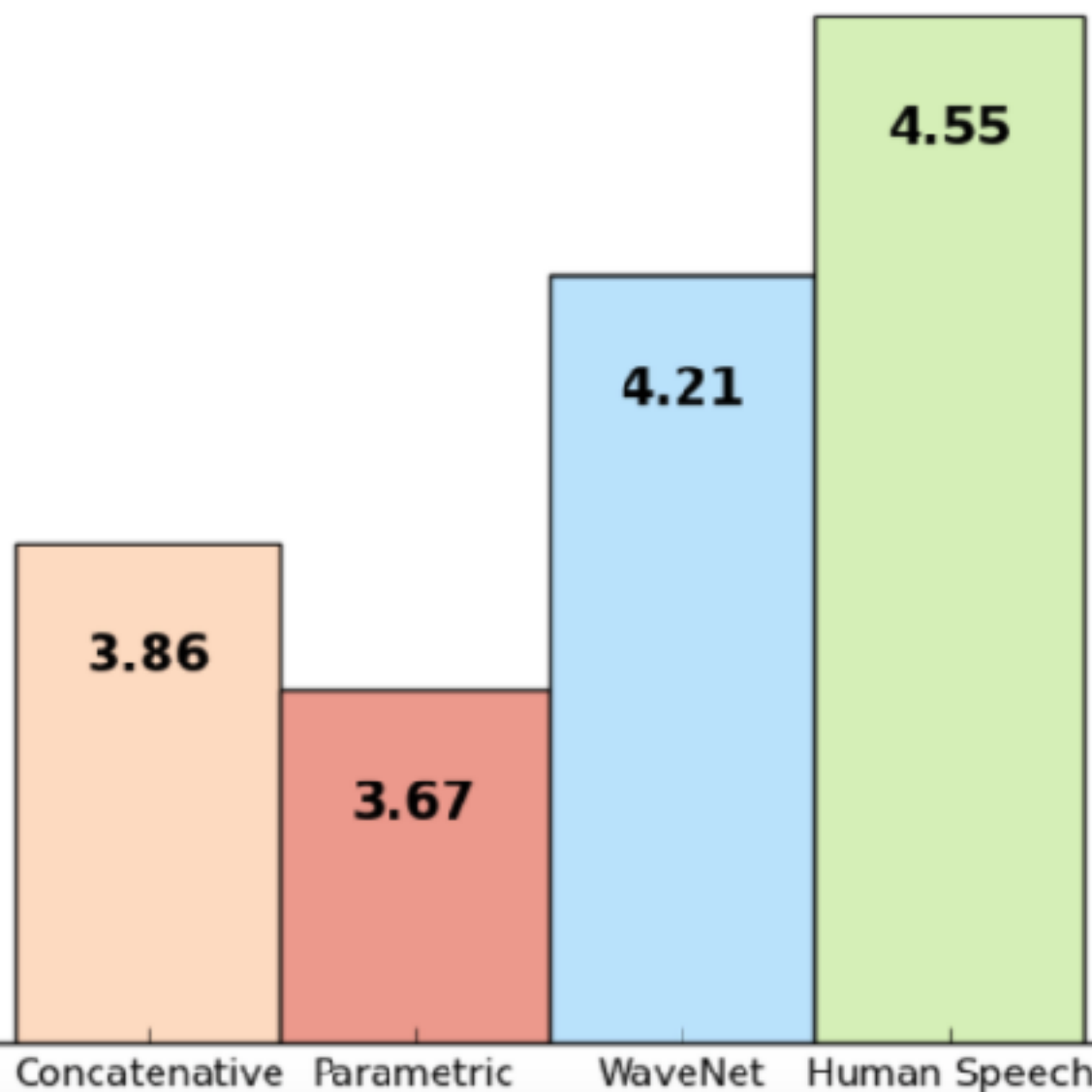


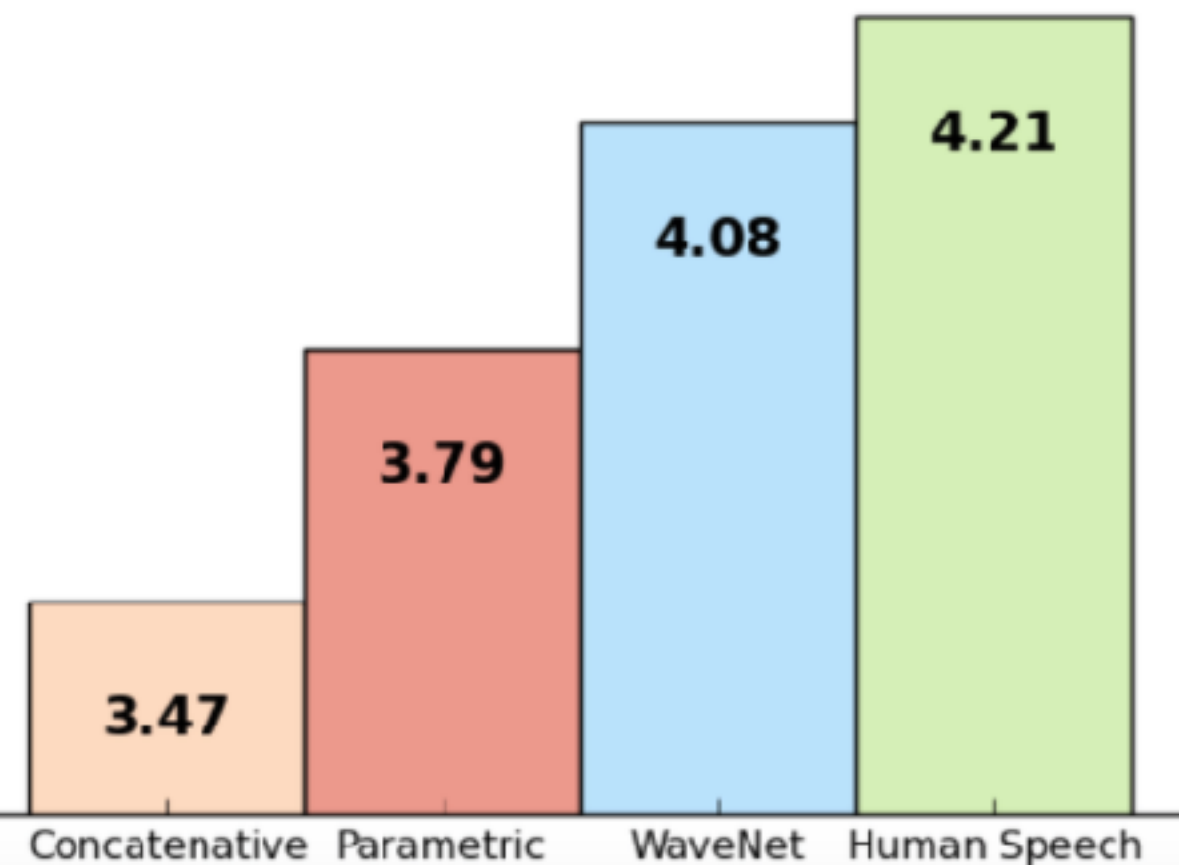
Figure 3: Visualization of a stack of *dilated* causal convolutional layers.

# WaveNet

US English



Mandarin Chinese



Subjective preference scores (%) of speech samples

# WaveNet

<https://deepmind.com/blog/wavenet-generative-model-raw-audio/>

# Computer Aided Diagnosis in Medical Imaging

# Convnet for Brain Tumor Segmentation (Top 4 in BRATS 2015)

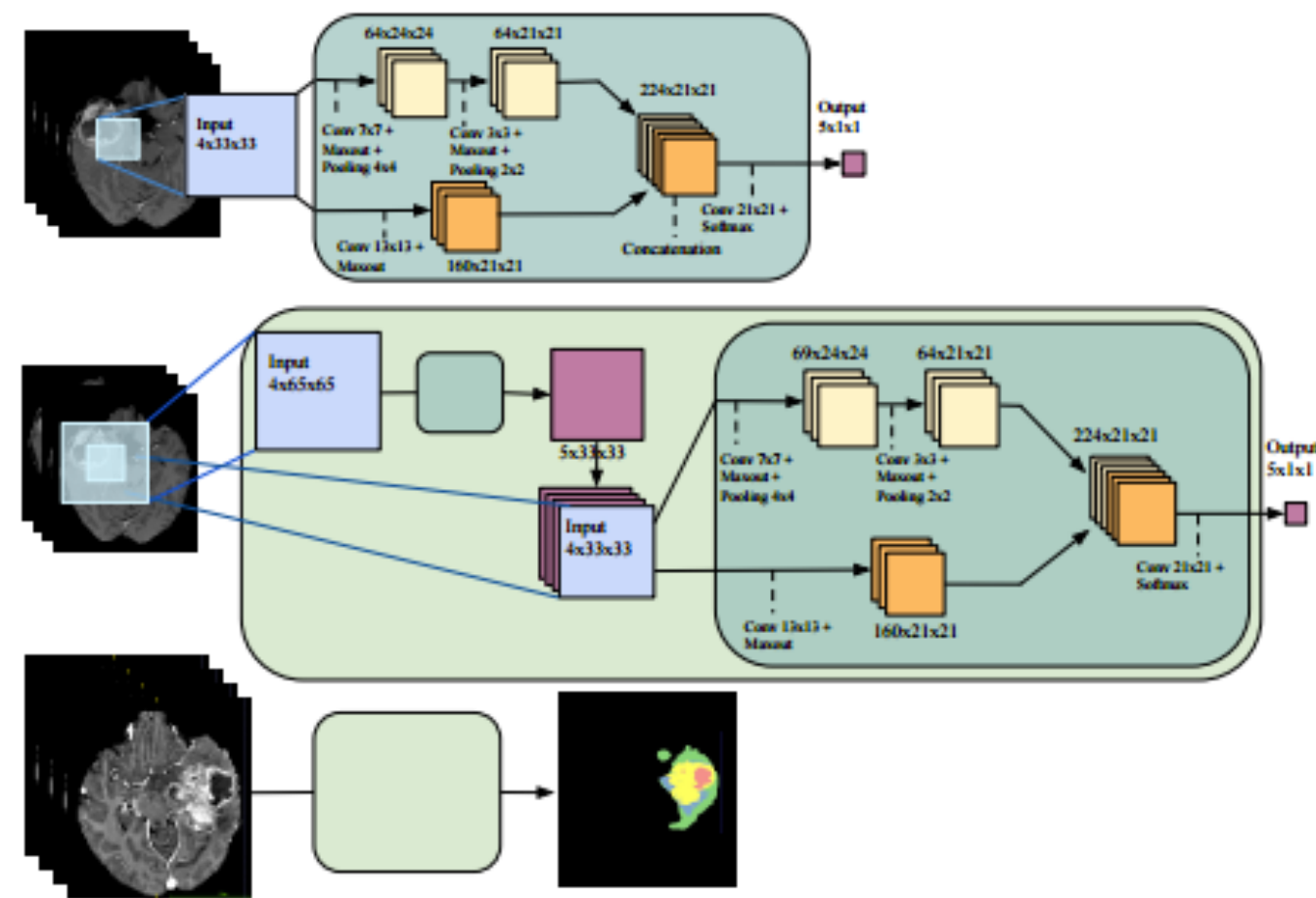
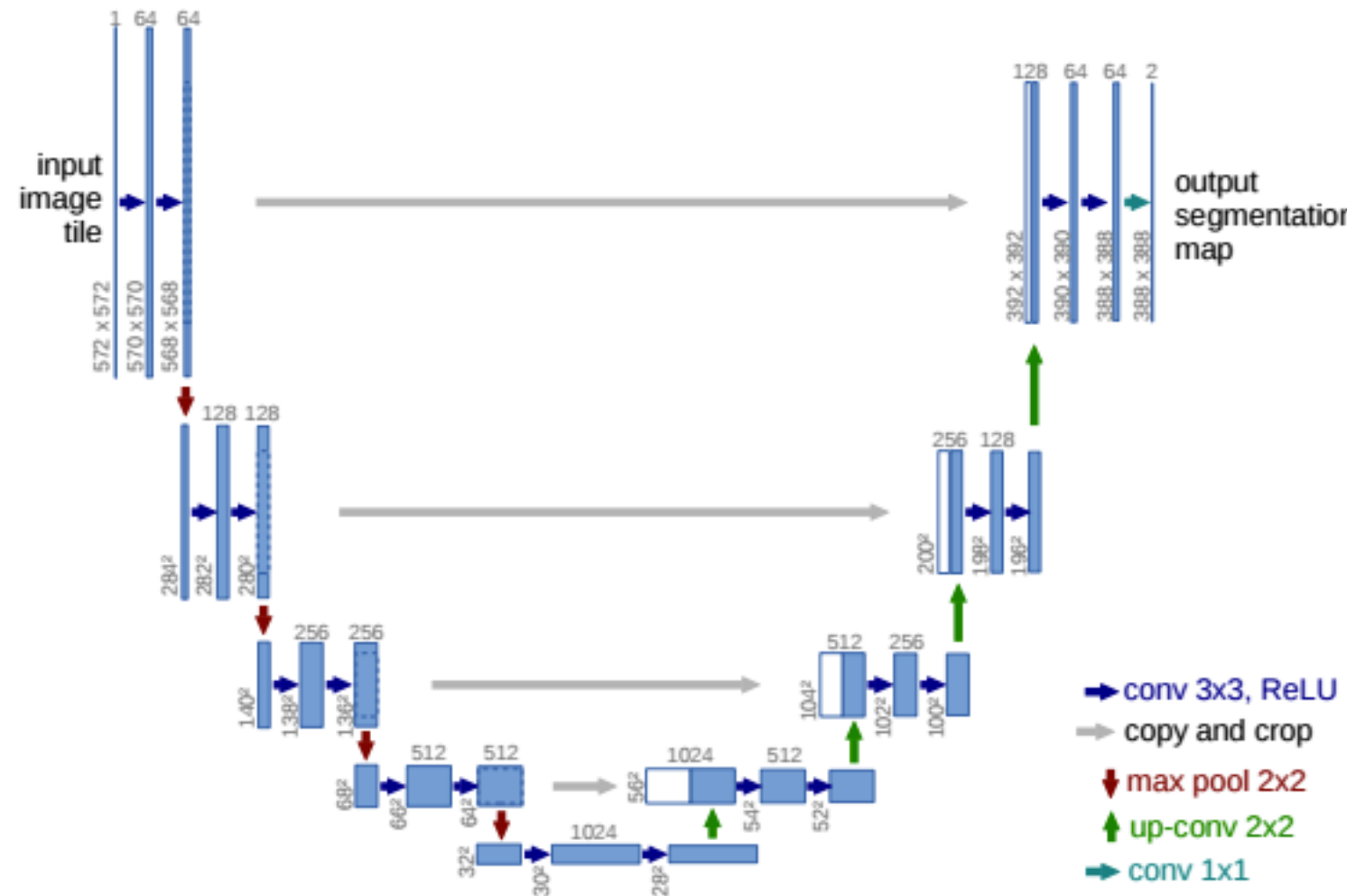


Fig. 1: The proposed architecture by Havaei et al. [35]. First row: TwoPATHCNN. The input patch goes through two convolutional networks each comprising of a local and a global path. The feature maps in the local and global paths are shown in yellow and orange respectively. Second row: INPUTCASCADECNN. The class probabilities generated by TwoPATHCNN are concatenated to the input of a second CNN model. Third row: Full image prediction using INPUTCASCADECNN.

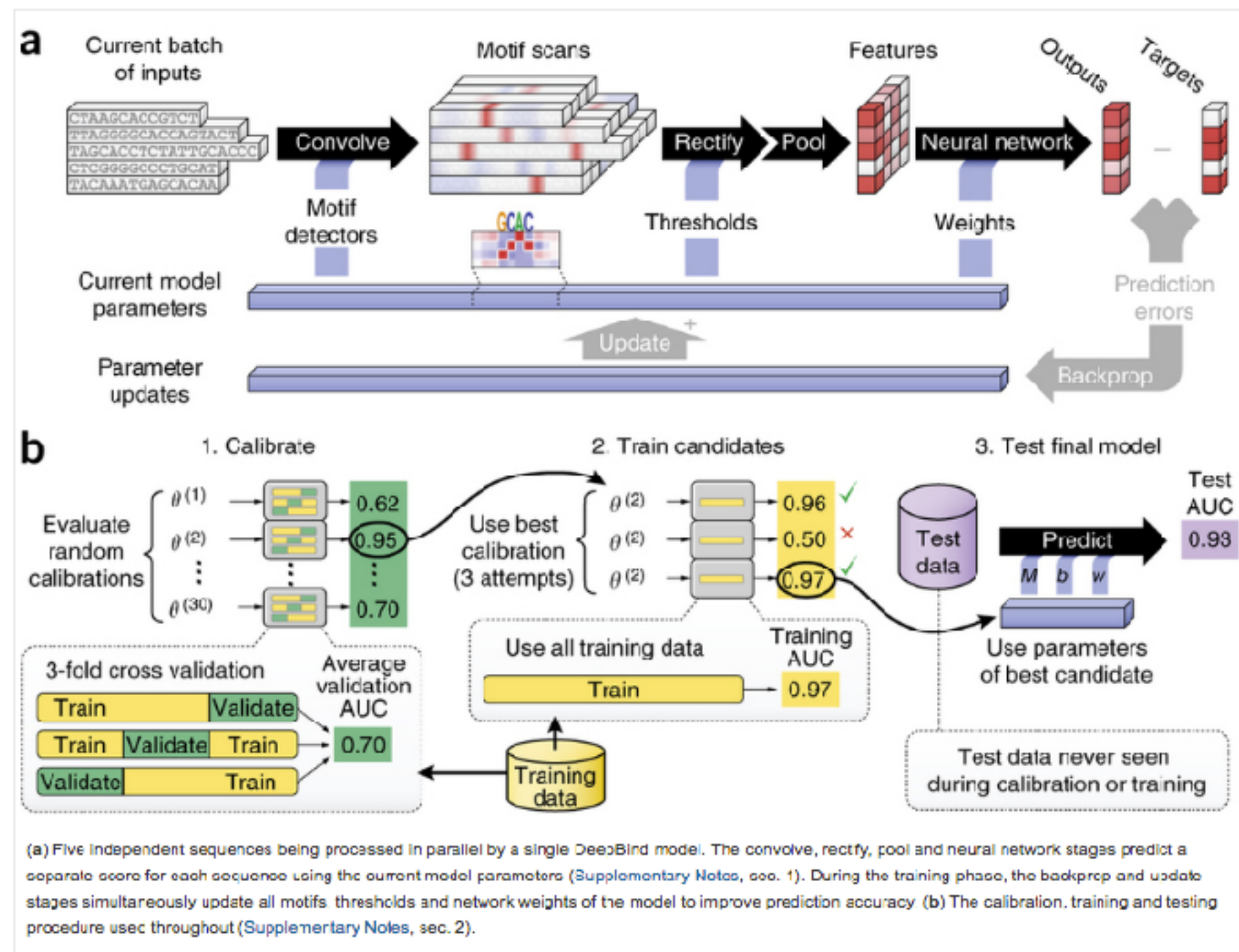
# U-Net: Convnet for Segmentation of Neuronal Structures in Electron Microscopic Stacks (Won the ISBI Cell Tracking Challenge 2015)



**Fig. 1.** U-net architecture (example for  $32 \times 32$  pixels in the lowest resolution). Each blue box corresponds to a multi-channel feature map. The number of channels is denoted on top of the box. The x-y-size is provided at the lower left edge of the box. White boxes represent copied feature maps. The arrows denote the different operations.

# Genetics

# DeepBind: Convnet for Predicting the Sequence Specificities of DNA- and RNA-Binding Proteins



# Fashion

# Neuroaesthetics in Fashion: Modeling the Perception of Fashionability

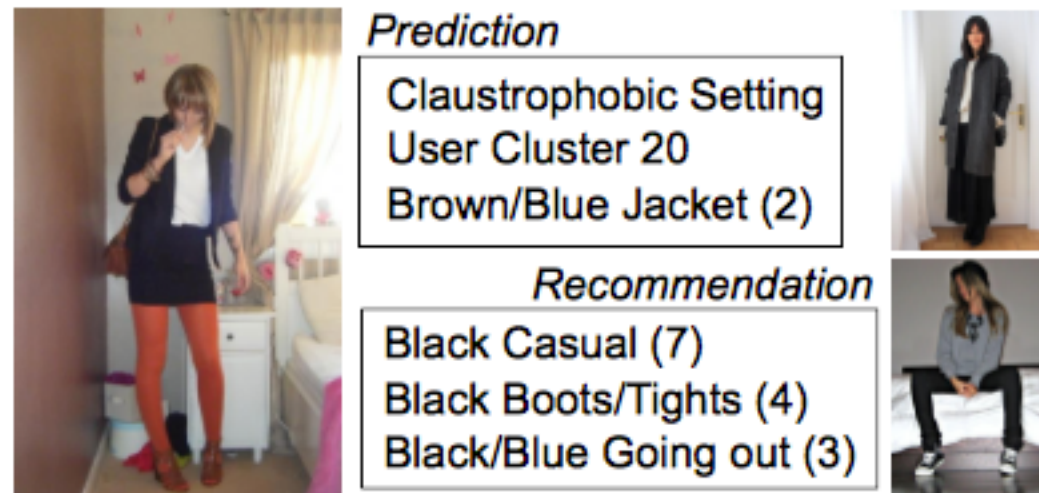


Figure 1: Example of recommendations provided by our model for the post on the left. In this case the user is wearing what we have identified as “Brown/Blue Jacket”. This photograph obtains a score of 2 out of 10 in fashionability. Additionally the user is classified as belonging to cluster 20 and took a picture in the “Claustrophobic” setting. If the user were to wear a “Black Casual” outfit as seen on the right, our model predicts she would improve her fashionability to 7 out of 10. This prediction is conditioned on the user, setting and other factors allowing the recommendations to be tailored to each particular user.

# Neuroaesthetics in Fashion: Modeling the Perception of Fashionability

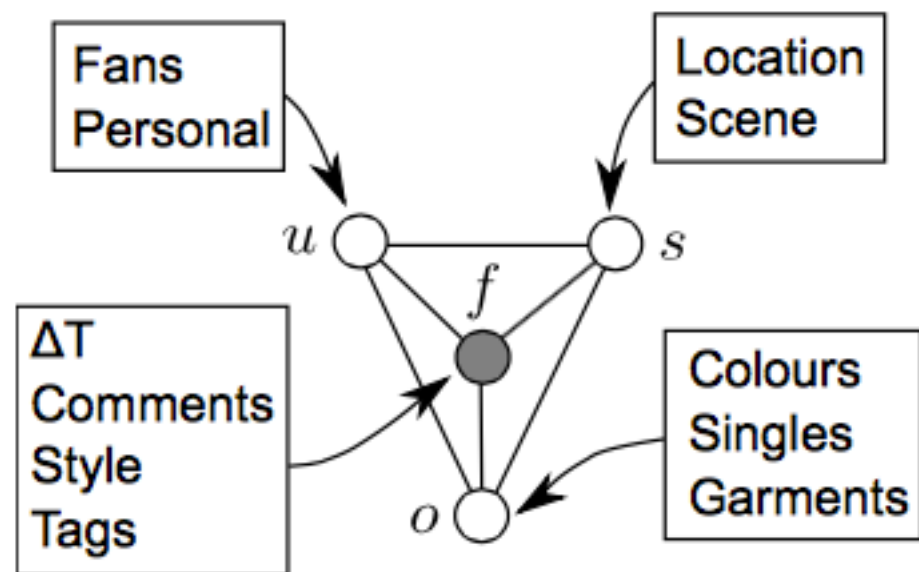


Figure 4: An overview of the CRF model and the features used by each of the nodes.

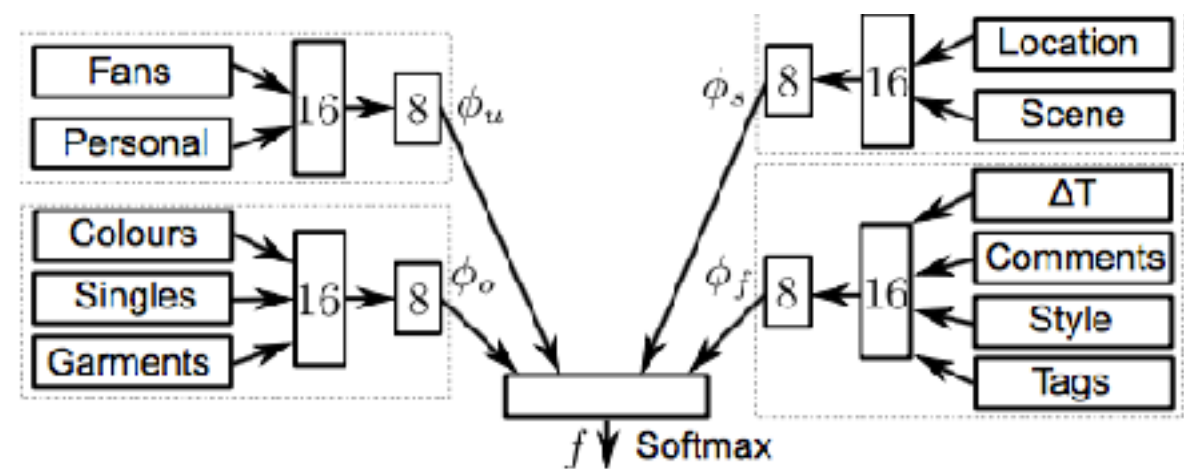


Figure 5: Illustration of the type of deep network architecture to learn features. We can see that it consists of four network joined together by a softmax layer. The output of the different networks  $\phi_f$ ,  $\phi_o$ ,  $\phi_u$ , and  $\phi_s$  are then used as features for the CRF.

# Neuroaesthetics in Fashion: Modeling the Perception of Fashionability

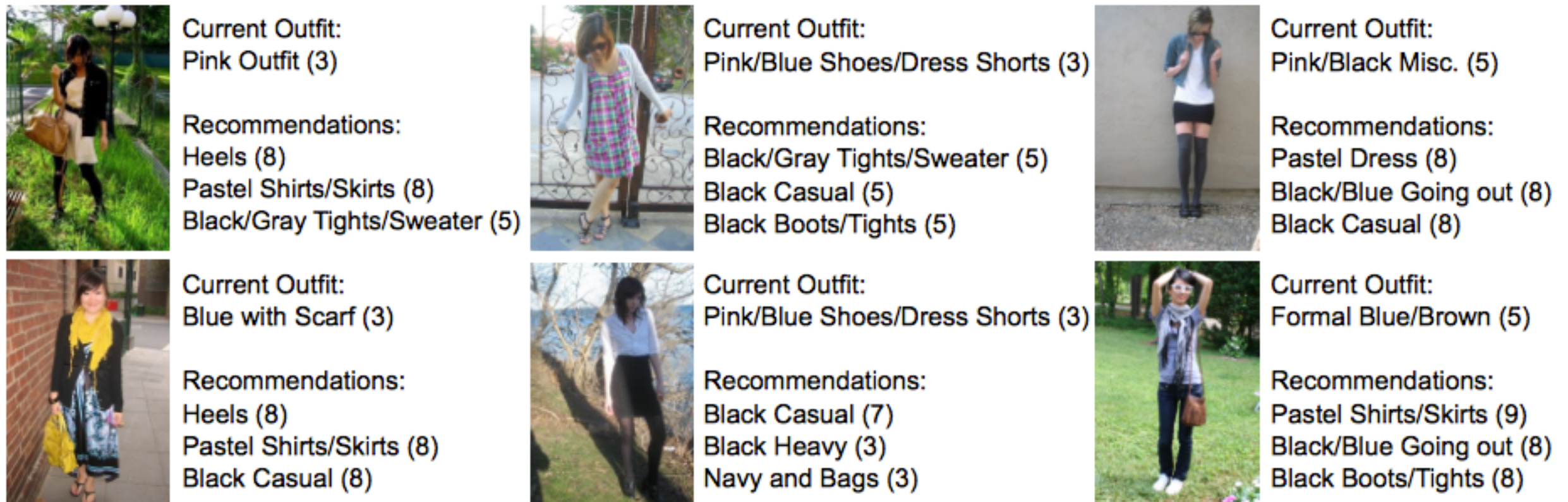
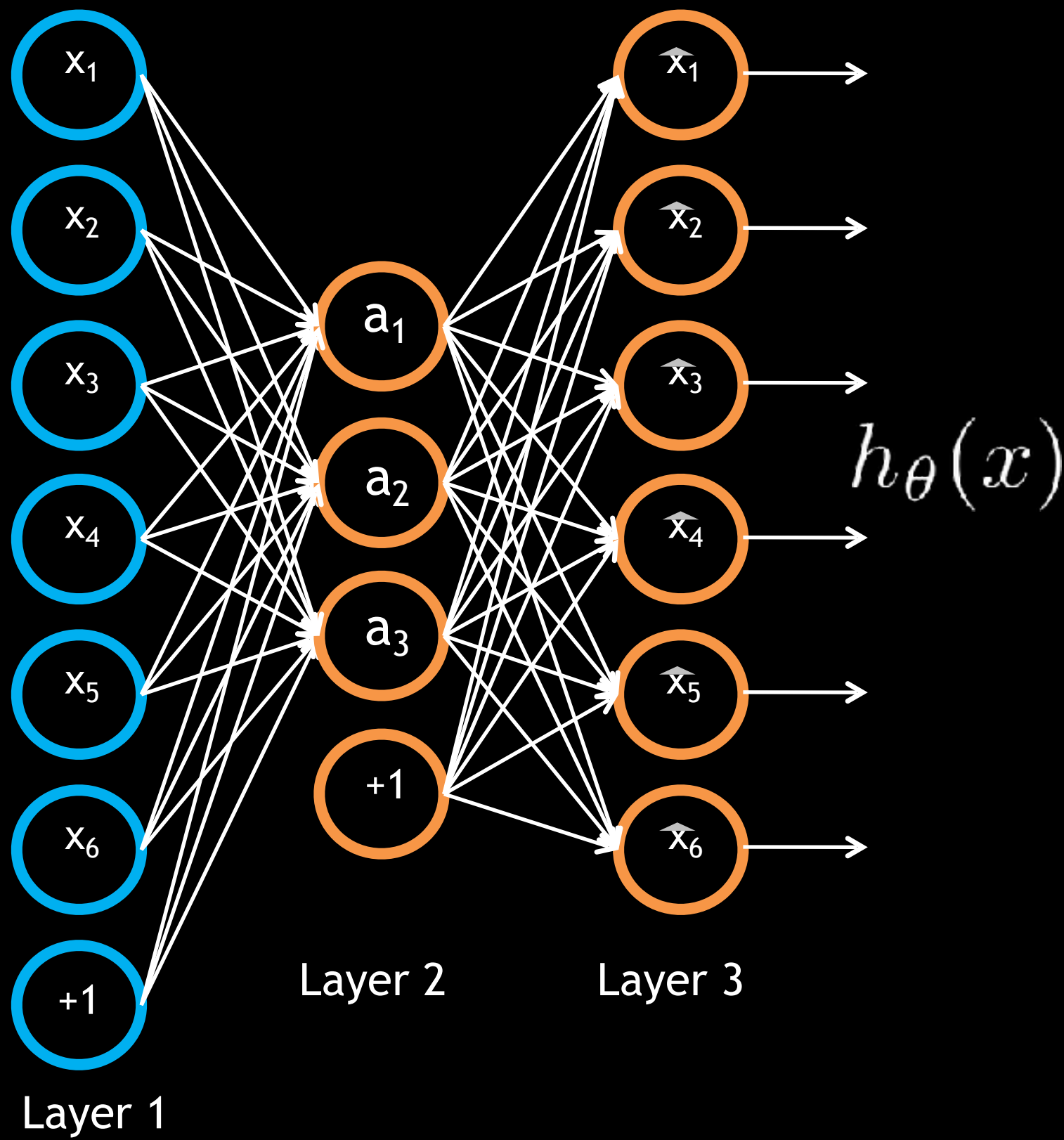


Figure 10: Example of recommendations provided by our model. In parenthesis we show the predicted fashionability.

## Unsupervised feature learning with a neural network



Autoencoder.

Network is trained to output the input (learn identity function).

$$h_{\theta}(x) \approx x$$

Trivial solution unless:

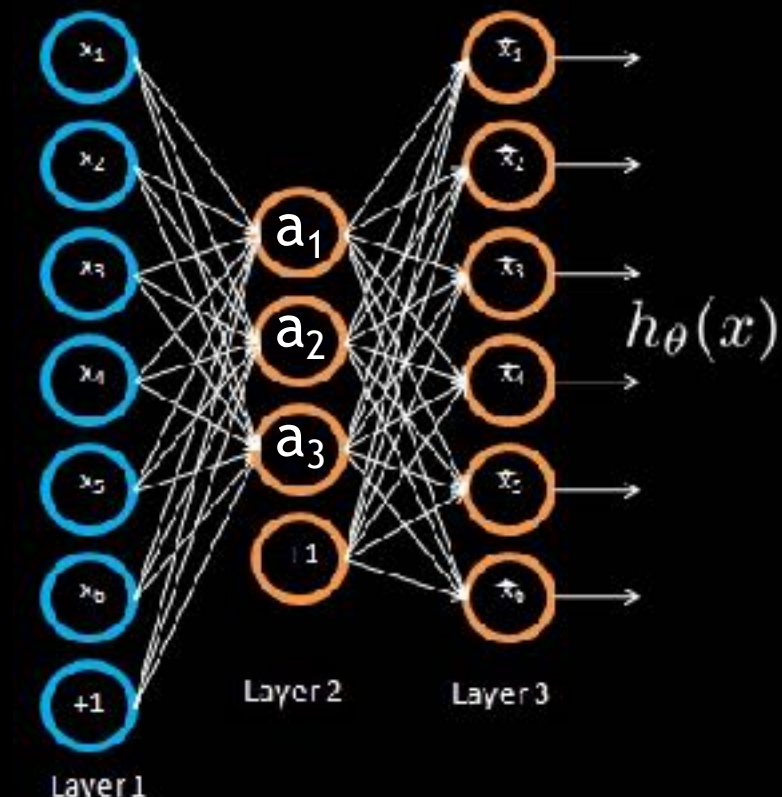
- Constrain number of units in Layer 2 (learn compressed representation), or
- Constrain Layer 2 to be **sparse**.

## Unsupervised feature learning with a neural network

Training a sparse autoencoder.

Given unlabeled training set  $x_1, x_2, \dots$

$$\min_{\theta} \underbrace{\|h_{\theta}(x) - x\|^2}_{\text{Reconstruction error term}} + \lambda \sum_i |a_i|$$



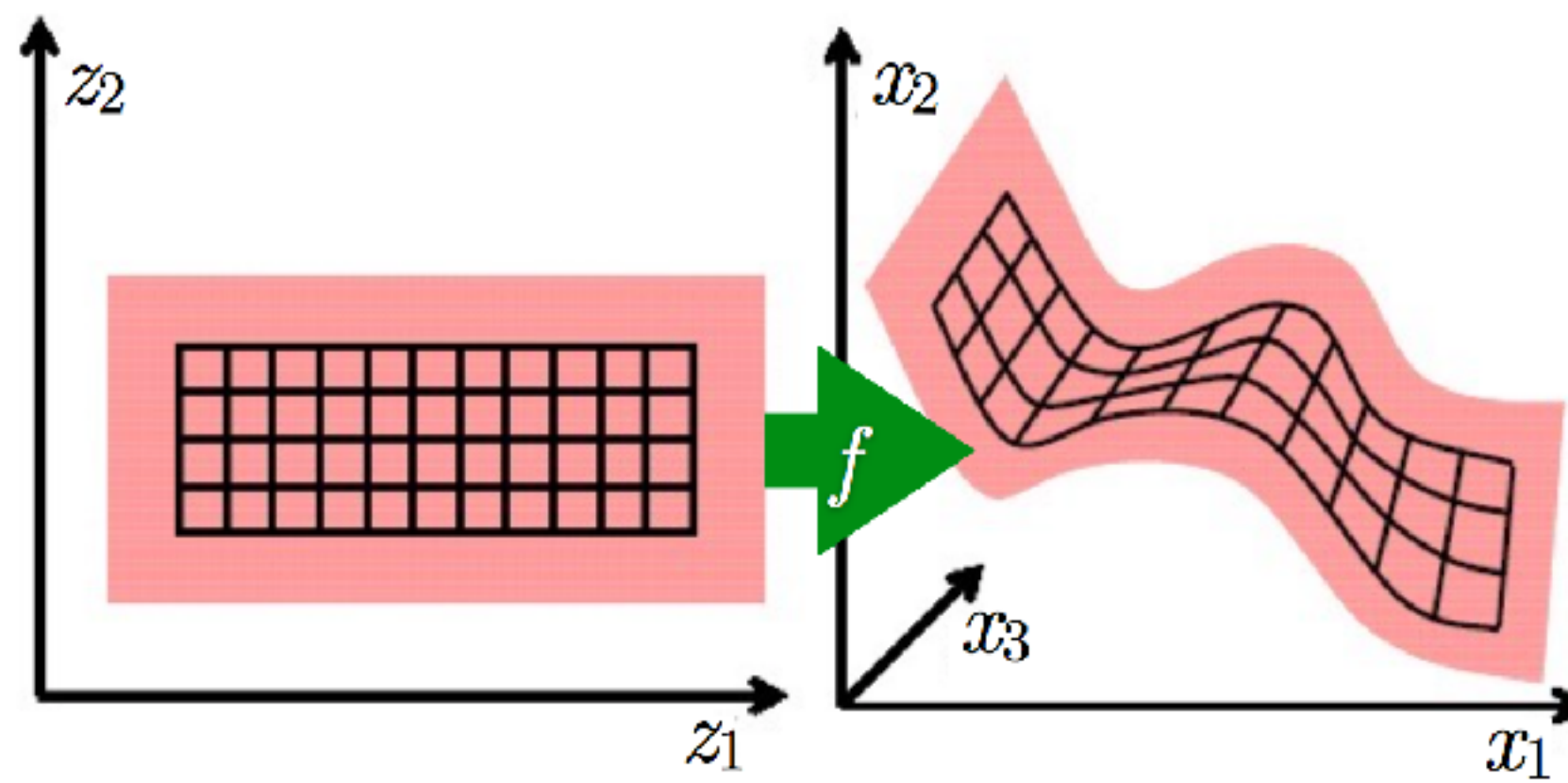
Reconstruction error    L<sub>1</sub> sparsity term  
term

# Variational Autoencoder

- **latent variable model:** learn a mapping from some latent variable  $z$  to a complicated distribution on  $x$ .

$$p(x) = \int p(x, z) dz \quad \text{where} \quad p(x, z) = p(x | z)p(z)$$
$$p(z) = \text{something simple} \quad p(x | z) = f(z)$$

- Can we learn to decouple the true **explanatory factors** underlying the data distribution? E.g. separate identity and expression in face images

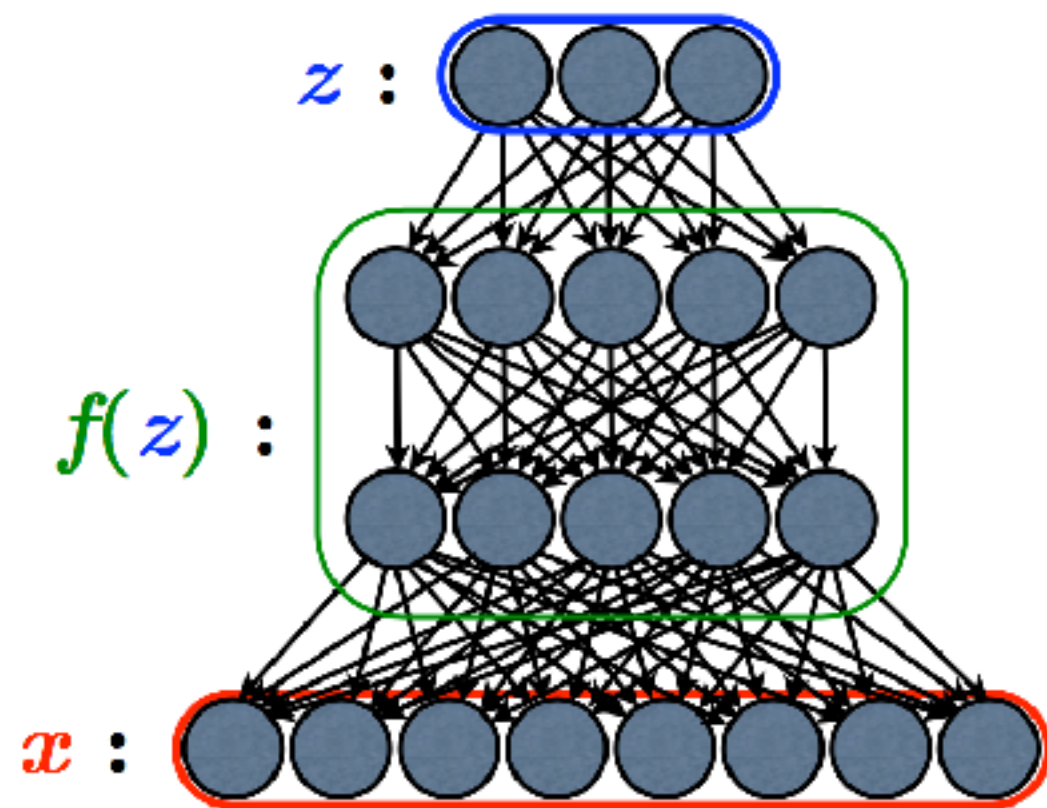
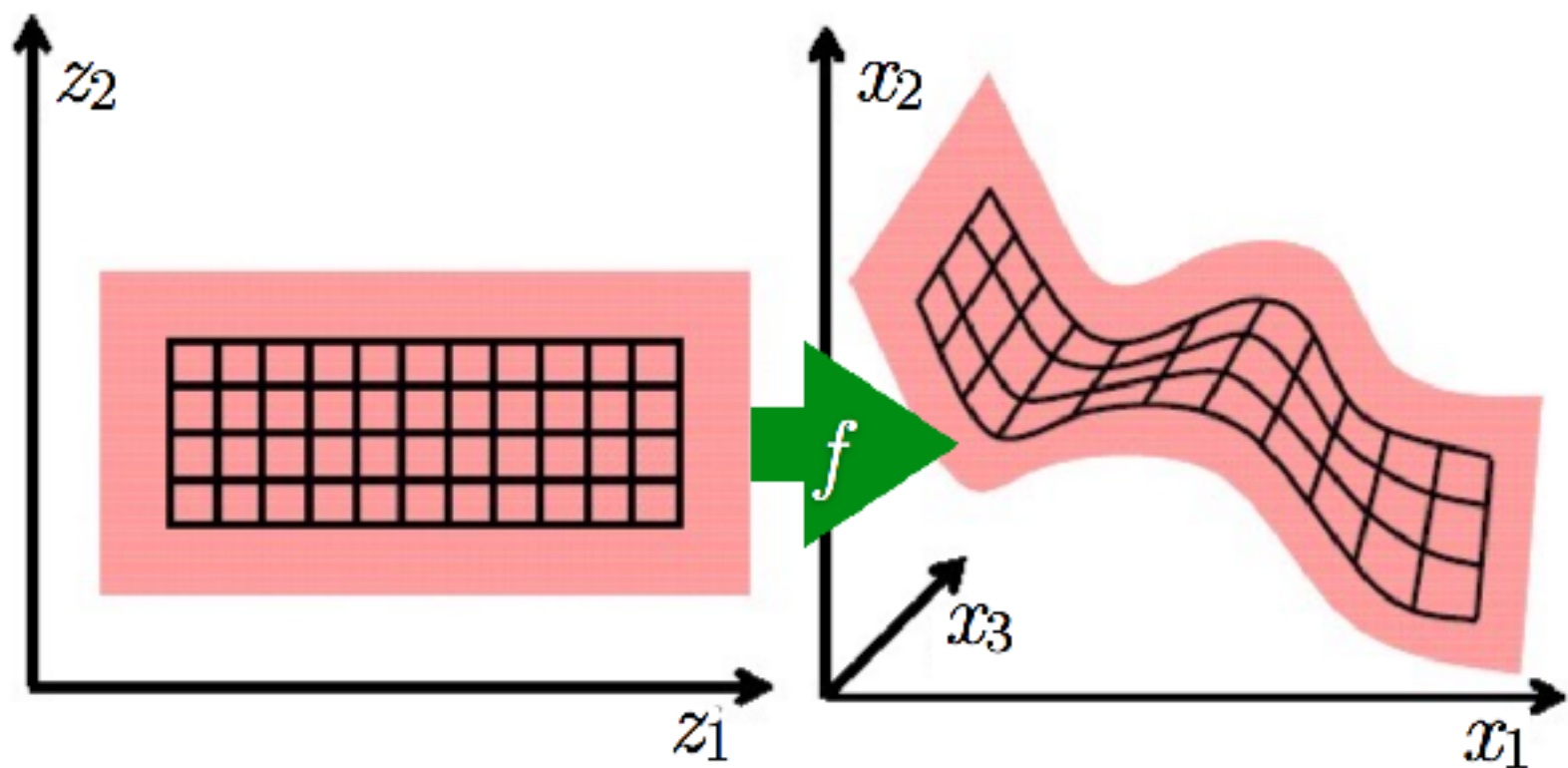


# Variational Autoencoder

- Leverage **neural networks** to learn a **latent variable model**.

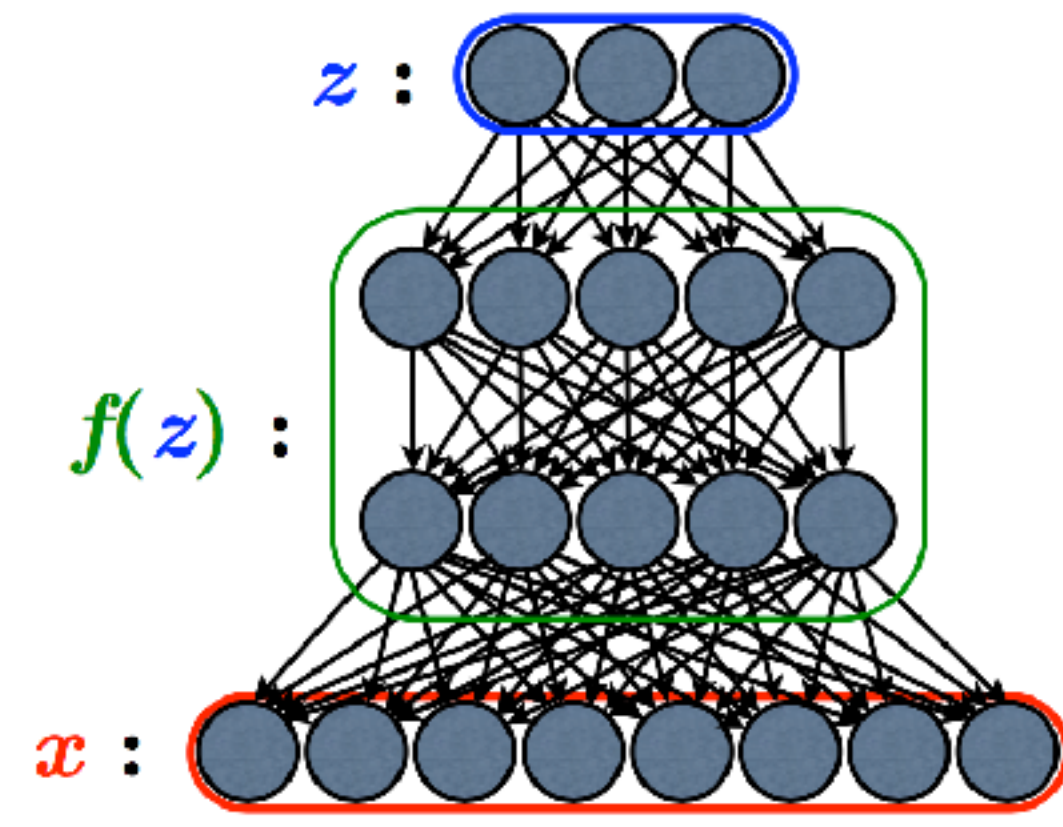
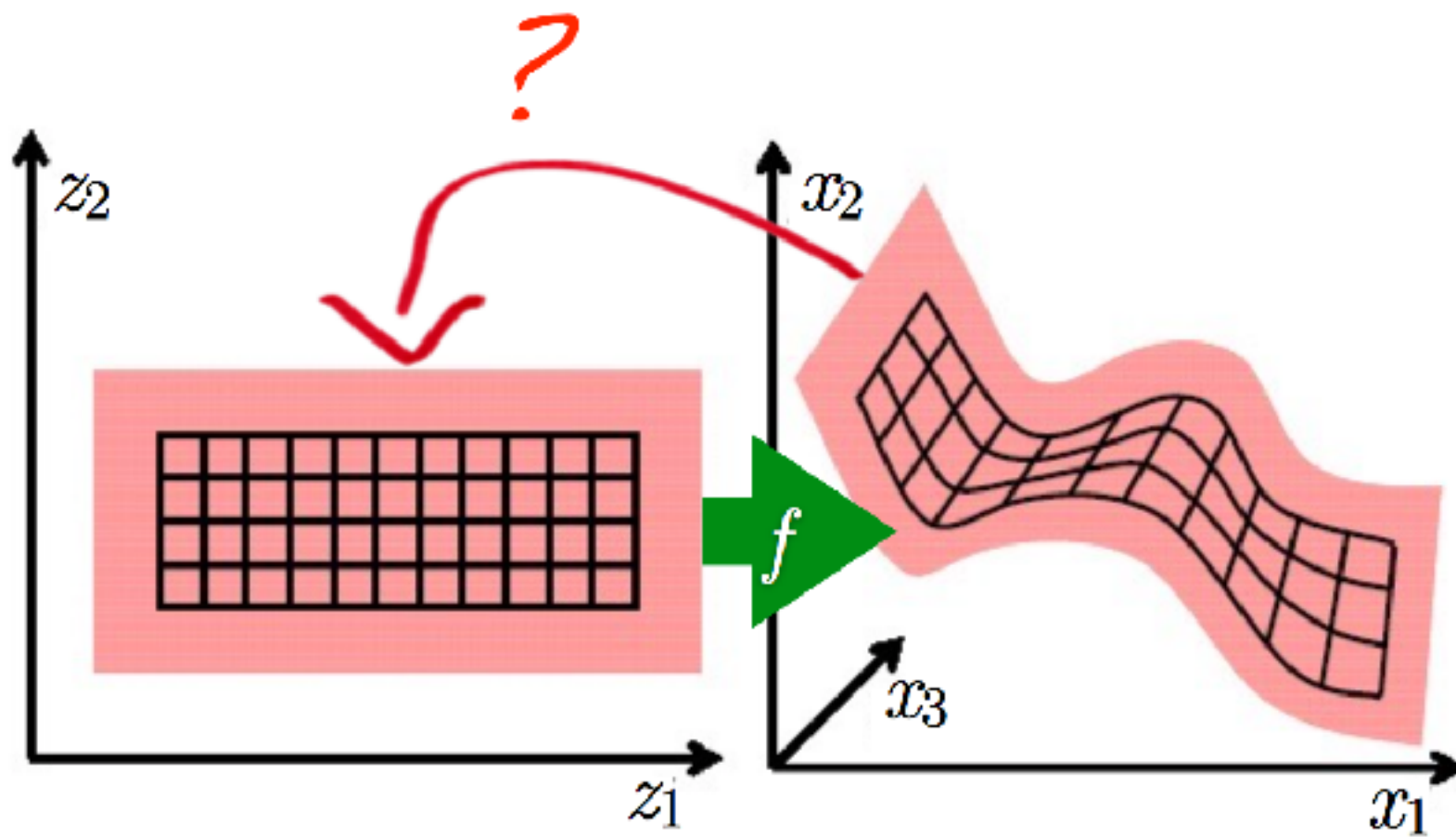
$$p(x) = \int p(x, z) dz \quad \text{where} \quad p(x, z) = p(x | z)p(z)$$

$$p(z) = \text{something simple} \quad p(x | z) = f(z)$$



# Inference/Learning Challenge

- **Where does  $z$  come from?** — The classic directed model dilemma.
- Computing the posterior  $p(z | x)$  is intractable.
- We need it to train the directed model.

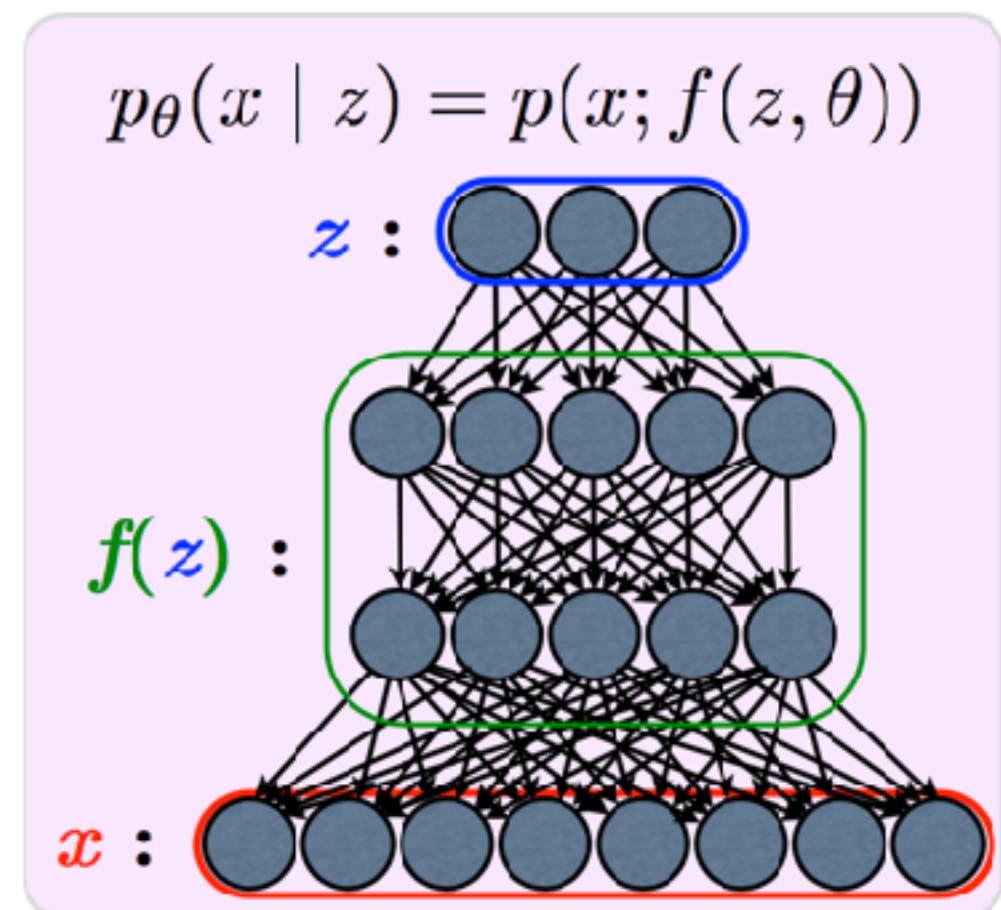
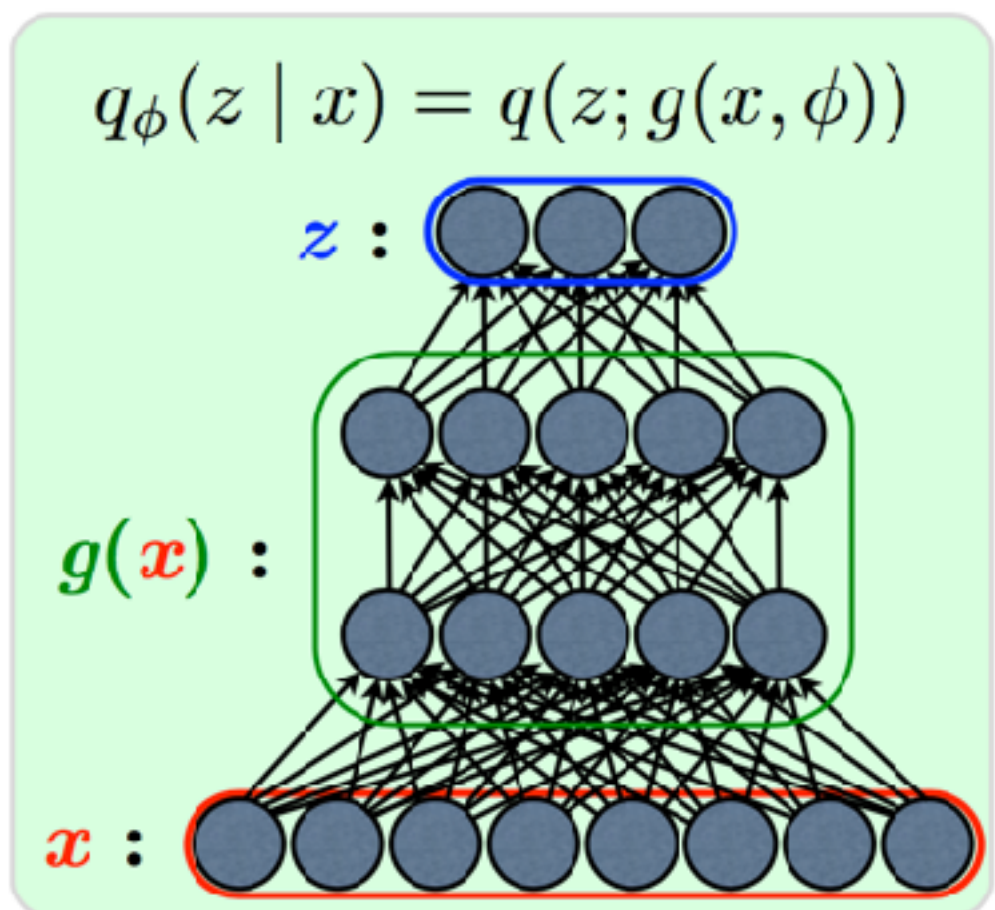


# Variational Autoencoder

- The **VAE approach**: introduce an inference model  $q_\phi(z | x)$  that **learns** to approximates the intractable posterior  $p_\theta(z | x)$  by optimizing the variational lower bound:

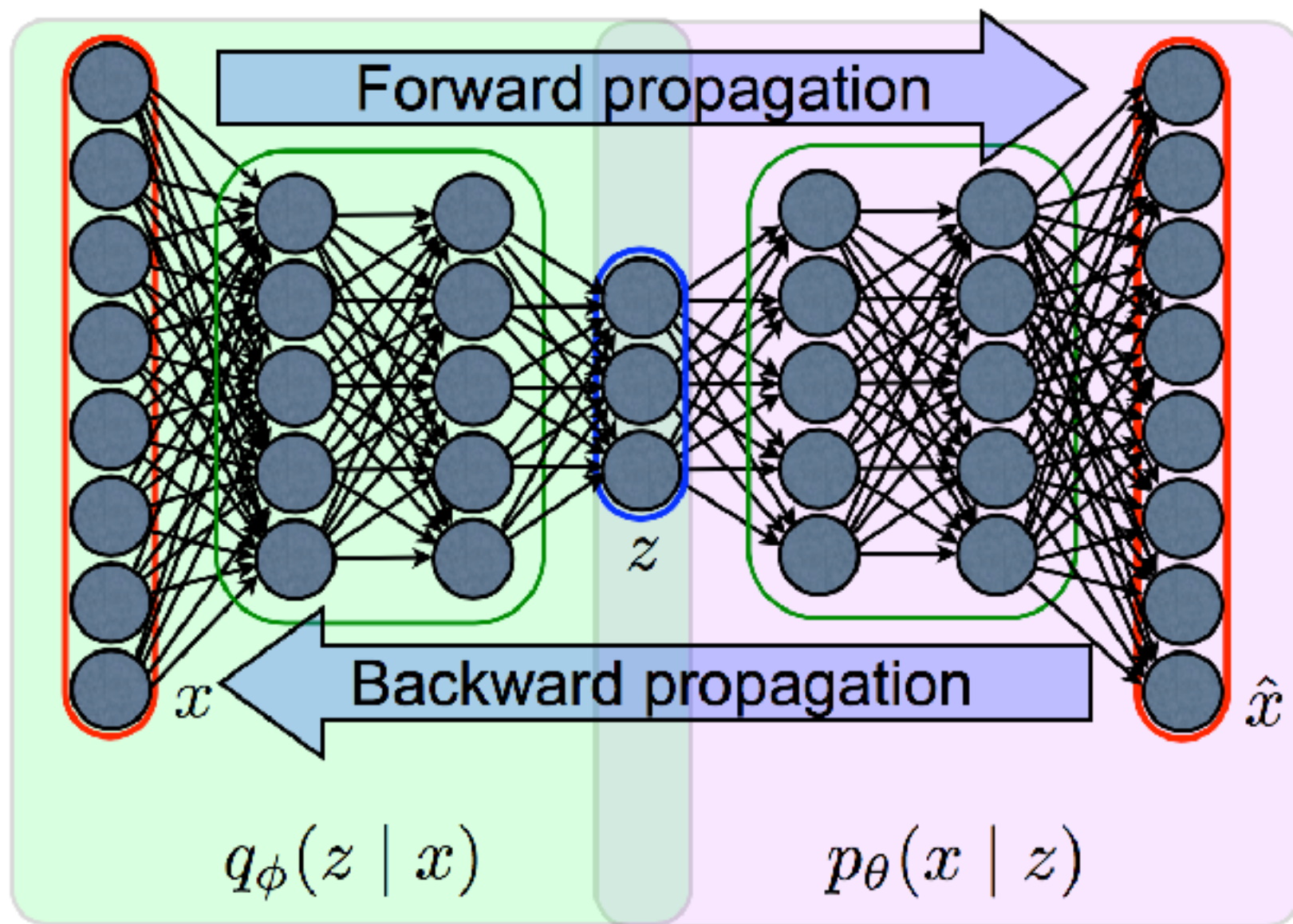
$$\mathcal{L}(\theta, \phi, x) = -D_{\text{KL}}(q_\phi(z | x) \| p_\theta(z)) + \mathbb{E}_{q_\phi(z|x)} [\log p_\theta(x | z)]$$

- We parameterize  $q_\phi(z | x)$  with another neural network:



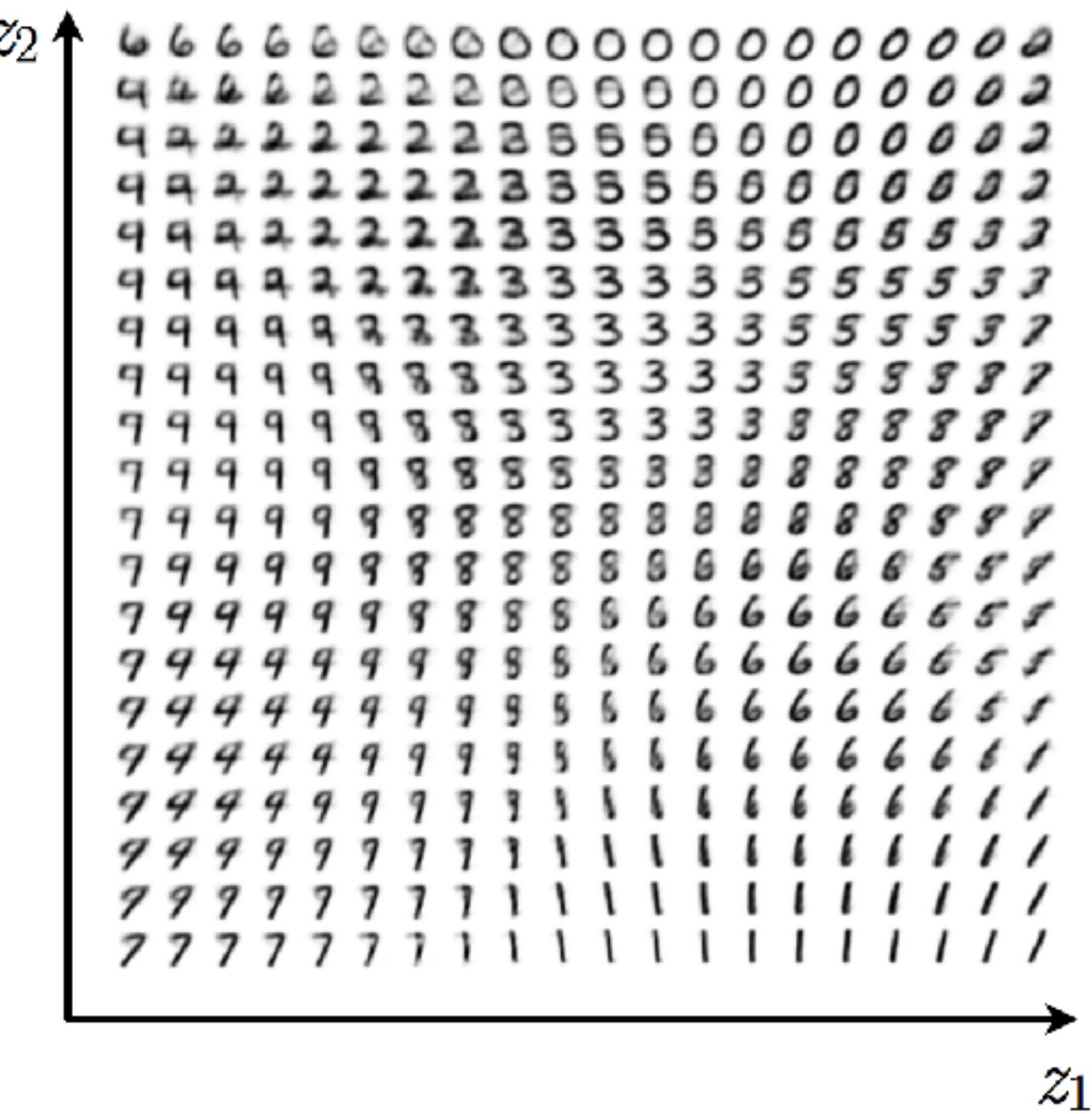
# Variational Autoencoder

Objective function:  $\mathcal{L}(\theta, \phi, x) = -D_{\text{KL}}(q_\phi(z | x) \| p_\theta(z)) + \mathbb{E}_{q_\phi(z|x)} [\log p_\theta(x | z)]$

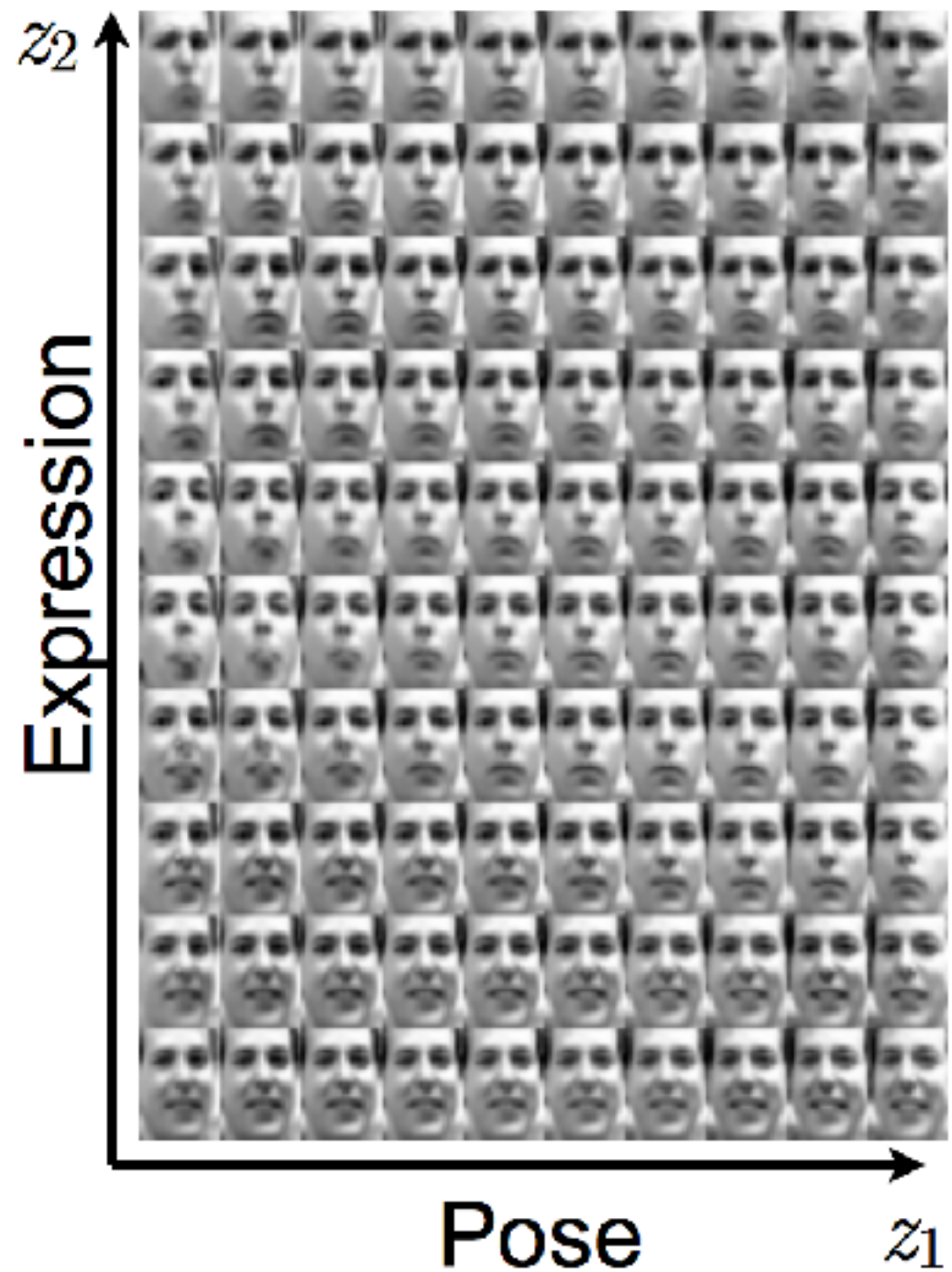


# Variational Autoencoder

MNIST:



Frey Face dataset:



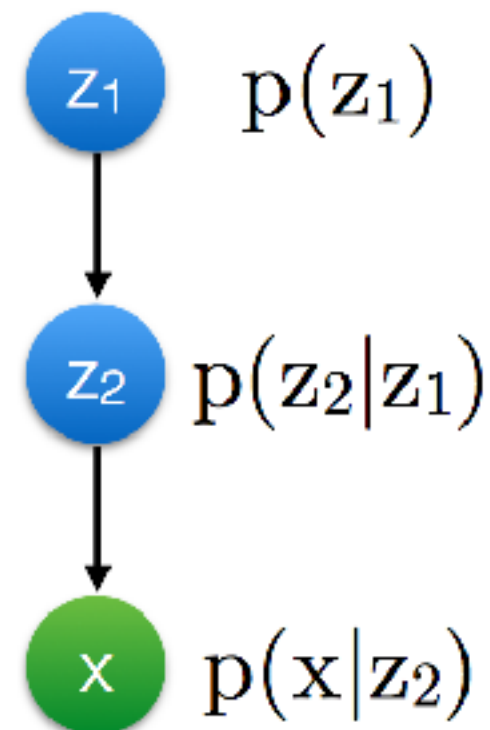
# Deep Latent-Variable Model

- We combining the strengths of **deep neural nets** with those of **latent-variable models**

- **directed latent variables models**: can represent complicated **marginal distributions** over  $x$

- probabilistic **deep neural nets**: can represent complicated conditional dependencies  $p(y|x) = f(x,y)$

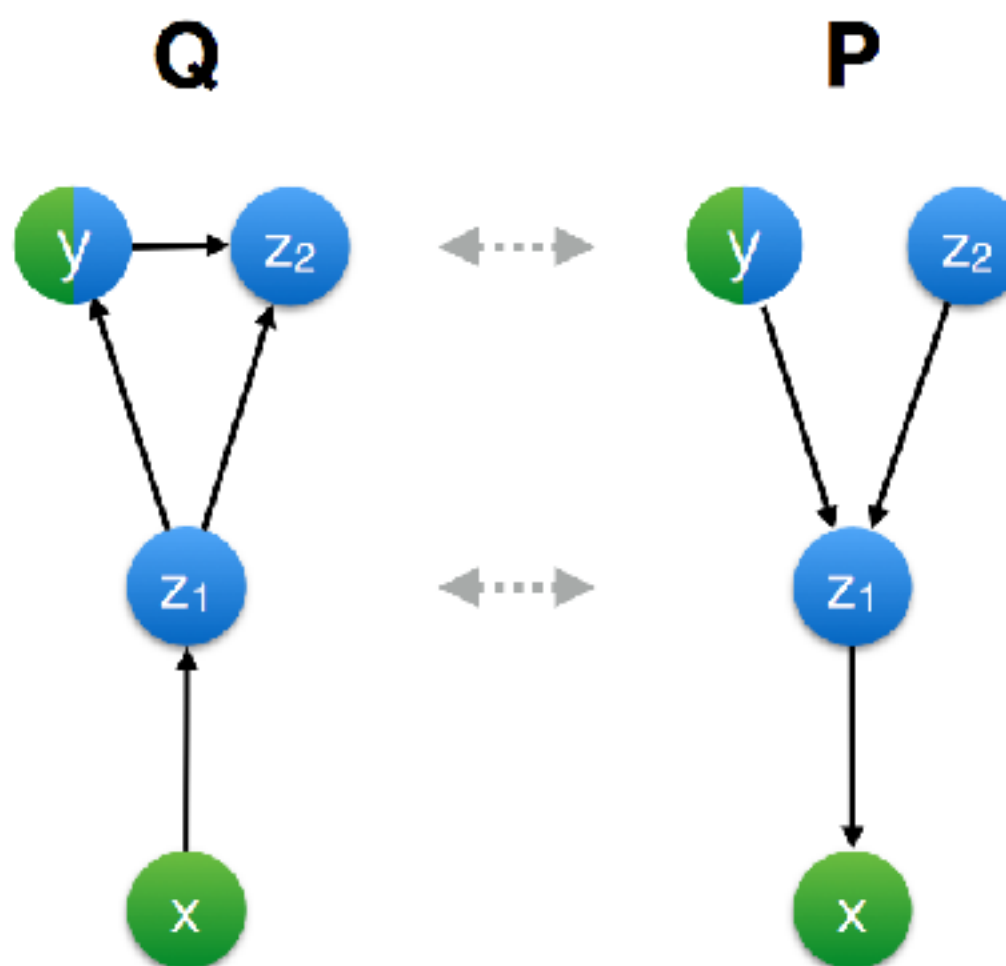
- Intractable posterior distribution  $p(z|x)$   
=> Approximate inference



$$p(x, z_1, z_2) = p(x|z_2)p(z_2|z_1)p(z_1)$$

# Deep Generative Model

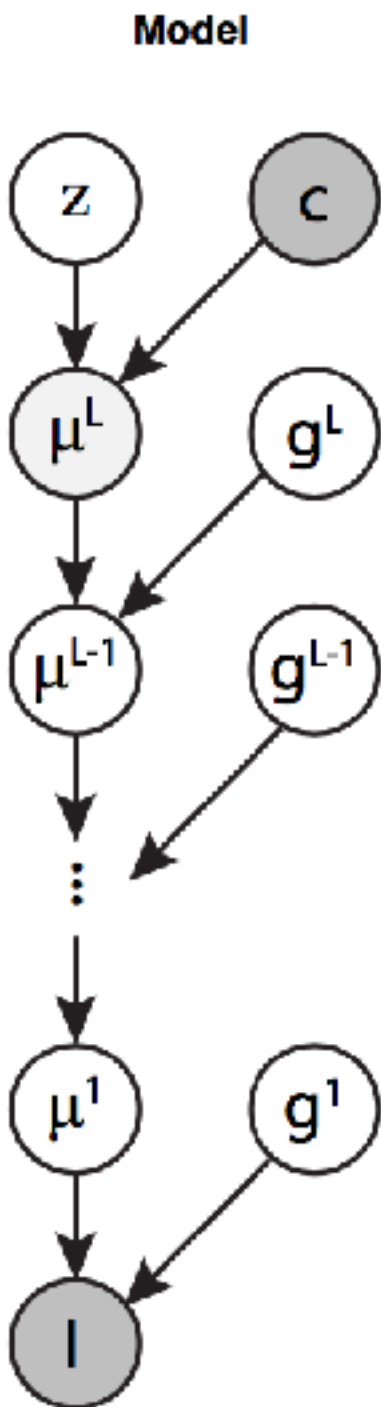
Stacked semi-supervised learner



Each edge is parameterised as a deep neural net

# Deep Rendering Model

Deep Rendering



E-step:

$$g_n^*, a_n^* = \arg \max_{g,a} \gamma_{nga}$$

$$\mathbb{E}[\tilde{a}_n \odot \tilde{z}_n | g_n^*, I_n; \theta] = \tilde{\Lambda}_{g_n^*}^\dagger [\tilde{a}_n^*] I_n$$

M-step:

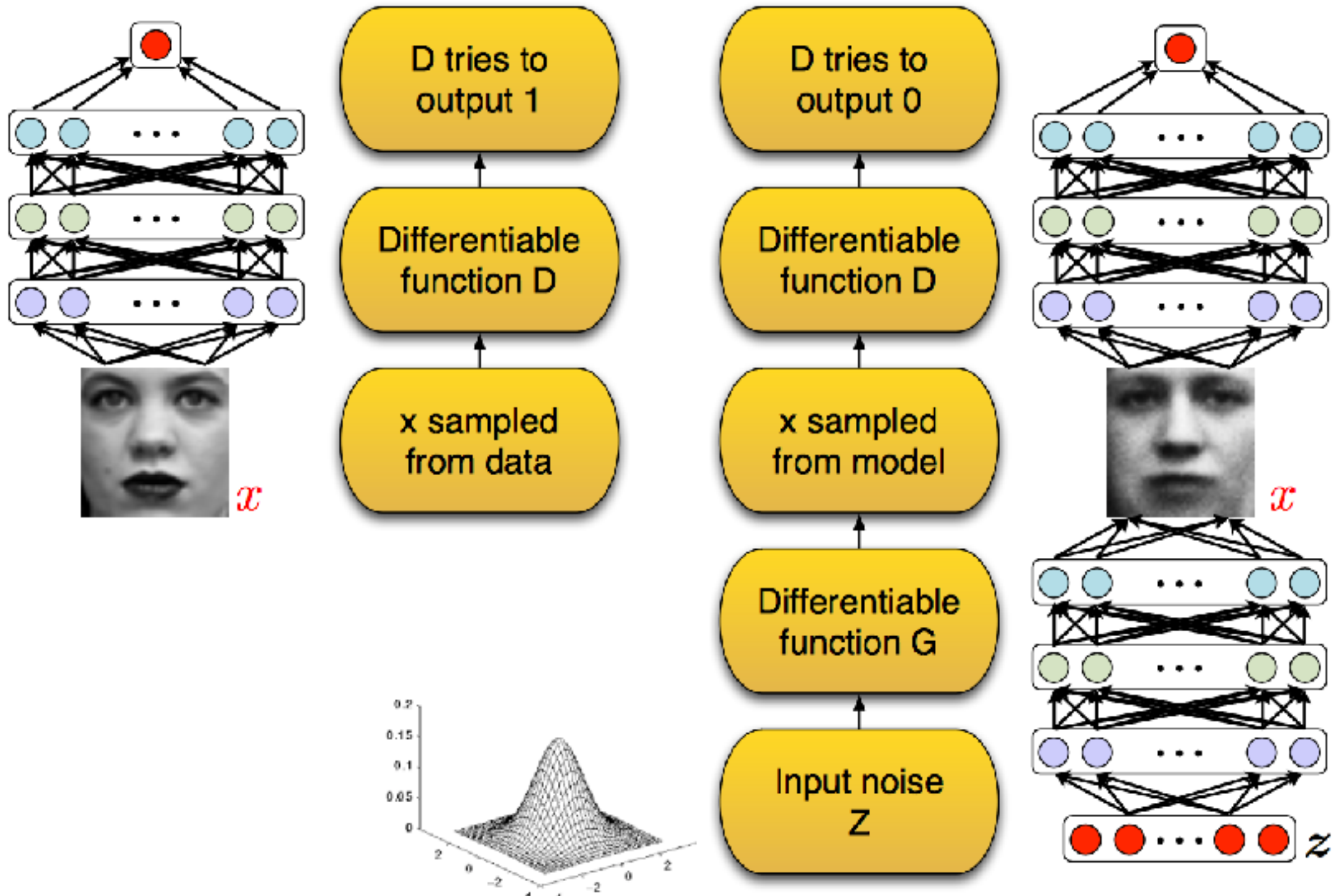
$$\tilde{\Lambda}_g = \text{OLS}(I_n \sim \mathbb{E}[\tilde{a}_n \odot \tilde{z}_n | g_n, I_n; \theta], n \in (g, a))$$

G-step:

$$\tilde{\Lambda}_g = \eta_{LR} \cdot \nabla_{\tilde{\Lambda}_g} \ell_{DRM}(\theta)$$



# Generative Adversarial Networks (GAN)



# Zero-Sum Game Objective

- Minimax objective function:

$$\min_G \max_D V(D, G) = \mathbb{E}_{\mathbf{x} \sim p_{\text{data}}(\mathbf{x})} [\log D(\mathbf{x})] + \mathbb{E}_{\mathbf{z} \sim p_{\mathbf{z}}(\mathbf{z})} [\log(1 - D(G(\mathbf{z})))]$$

- In practice, to estimate  $G$  we use:

$$\max_G \mathbb{E}_{\mathbf{z} \sim p_{\mathbf{z}}(\mathbf{z})} [\log D(G(\mathbf{z}))]$$

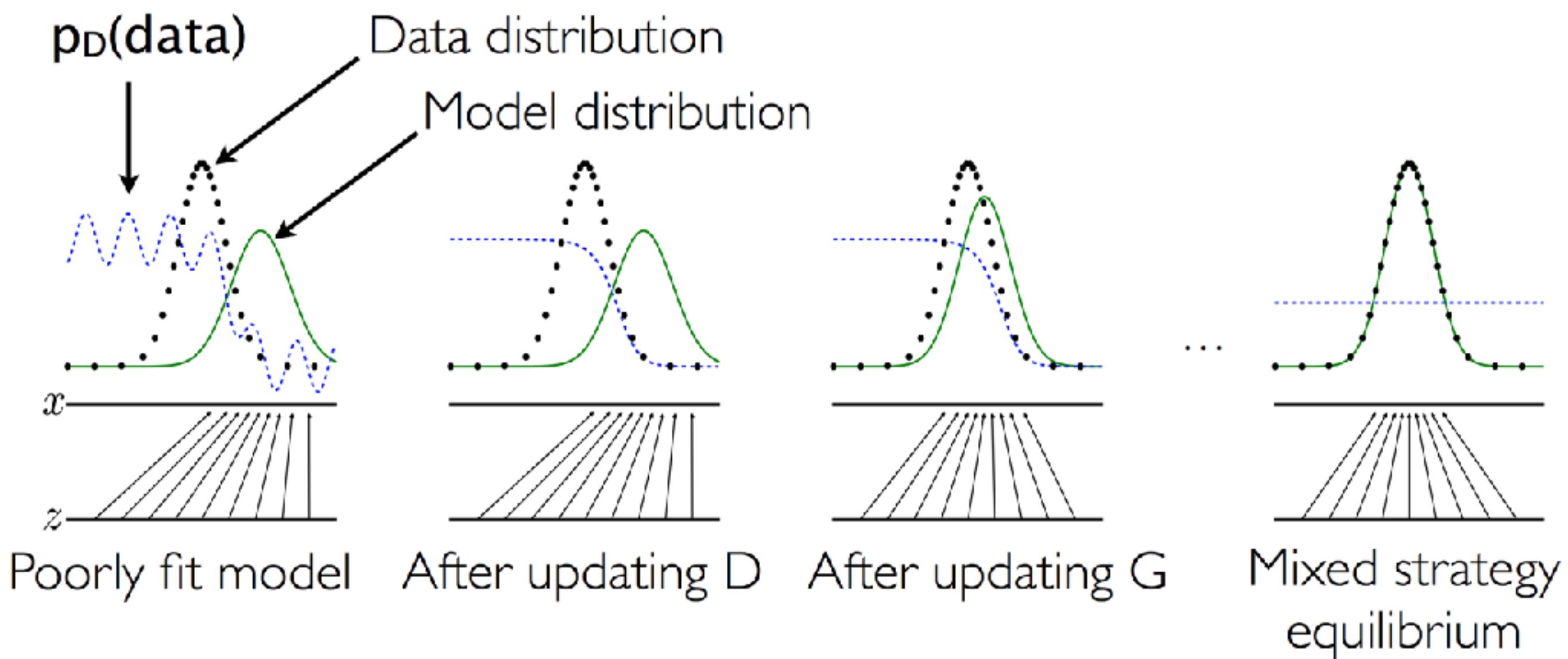
Why? Stronger gradient for  $G$  when  $D$  is very good.

# Zero-Sum Game Objective

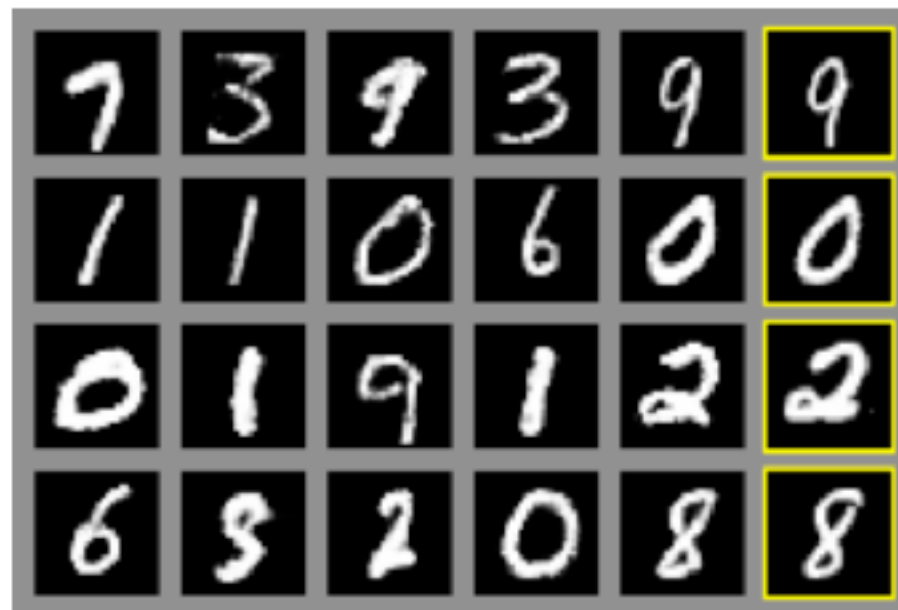
$$\min_G \max_D V(D, G) = \mathbb{E}_{\mathbf{x} \sim p_{\text{data}}(\mathbf{x})} [\log D(\mathbf{x})] + \mathbb{E}_{\mathbf{z} \sim p_{\mathbf{z}}(\mathbf{z})} [\log(1 - D(G(\mathbf{z})))]$$

- Theoretical properties (assuming infinite data, infinite model capacity, direct updating of generator's distribution):
  - Unique global optimum.
  - Optimum corresponds to data distribution.
  - Convergence to optimum guaranteed.

# Learning Process in GAN



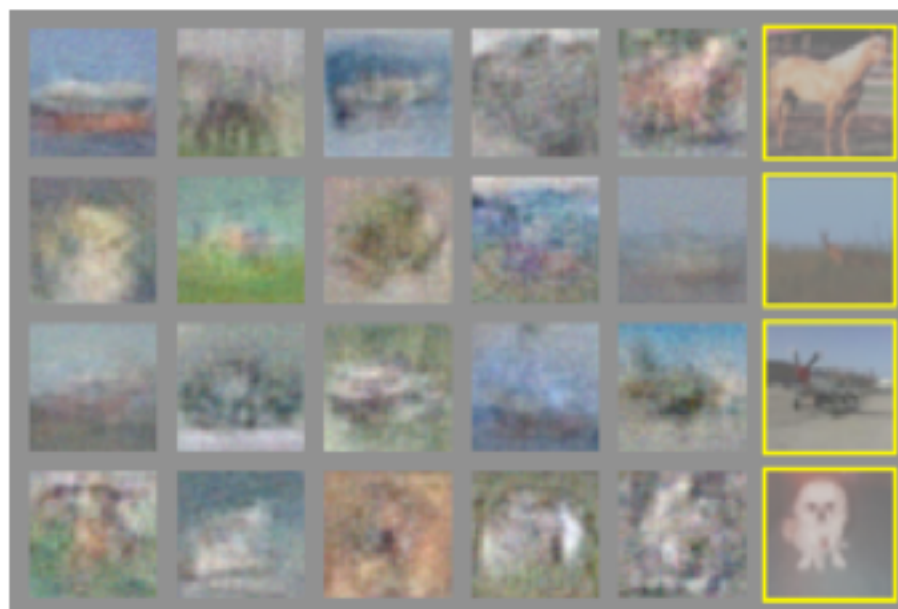
# Visualization of Model Samples



MNIST



TFD

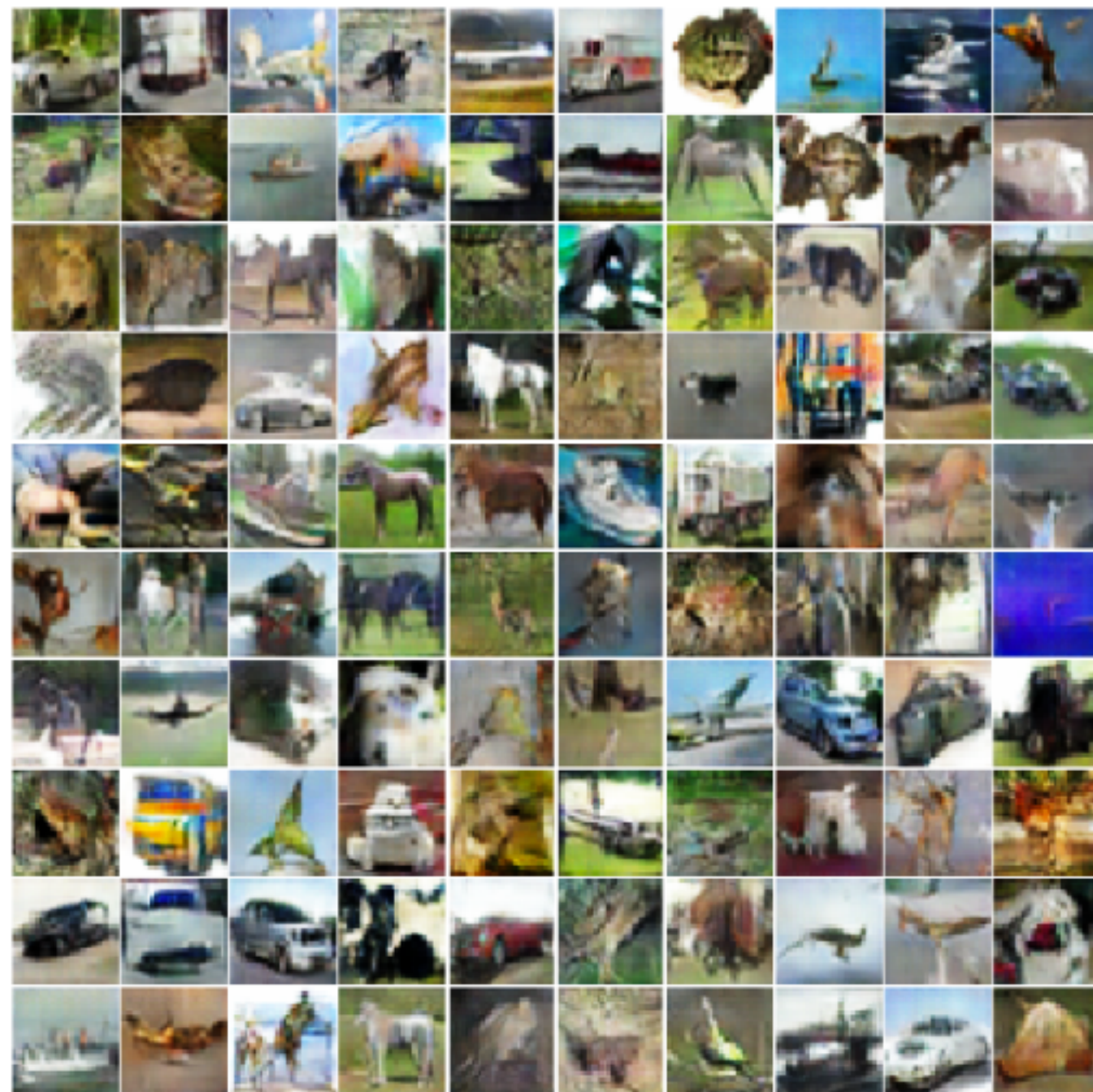


CIFAR-10 (fully connected)



CIFAR-10 (convolutional)

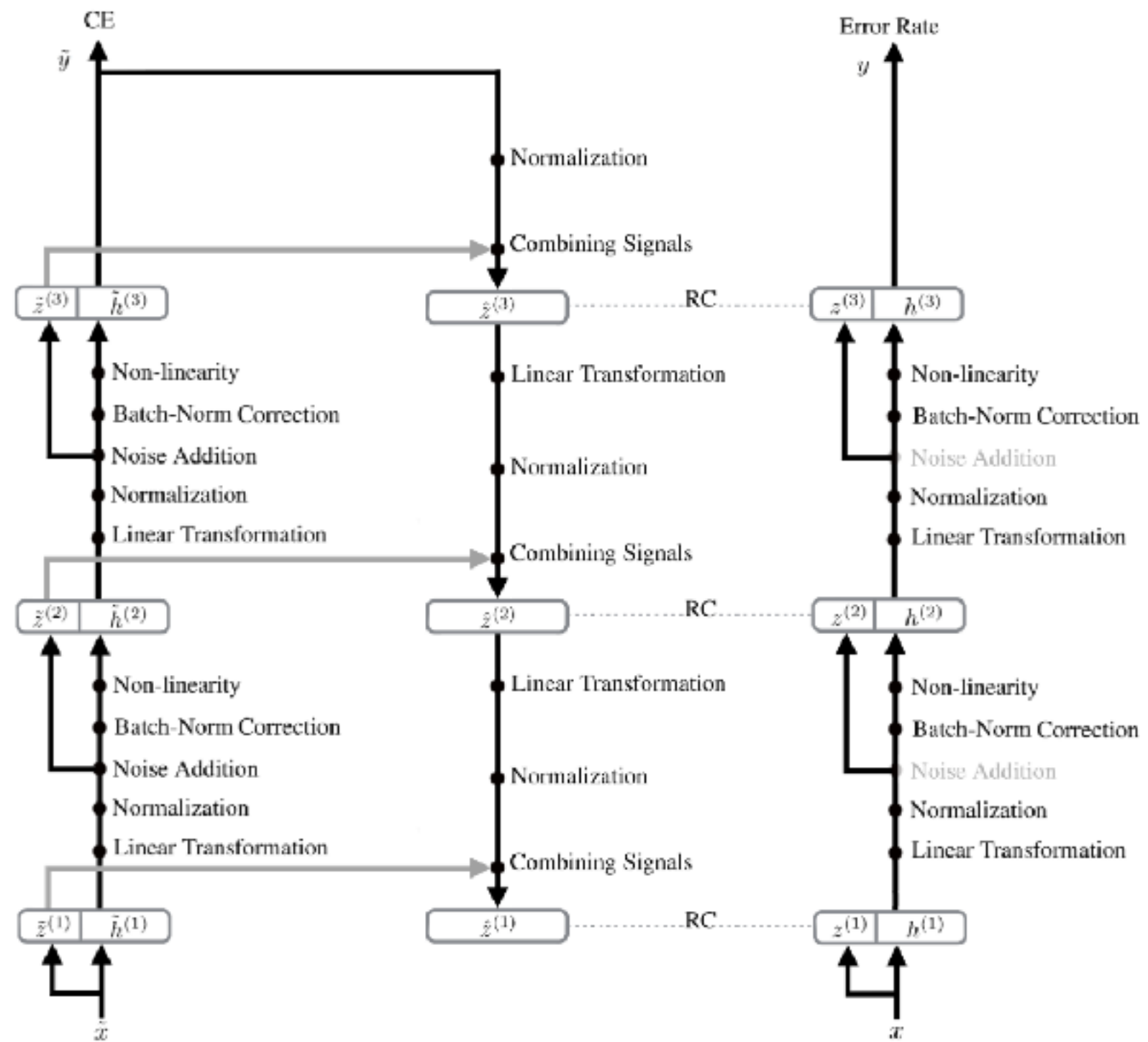
# Improved GAN



# Improved GAN



# Ladder Network



# Ladder Network

---

**Algorithm 1** Calculation of the output  $\mathbf{y}$  and cost function  $C$  of the Ladder network

---

```

Require:  $\mathbf{x}(n)$                                      # Final classification:  

# Corrupted encoder and classifier           $P(\mathbf{y} | \mathbf{x}) \leftarrow \mathbf{h}^{(L)}$   

 $\tilde{\mathbf{h}}^{(0)} \leftarrow \tilde{\mathbf{z}}^{(0)} \leftarrow \mathbf{x}(n) + \text{noise}$           # Decoder and denoising  

for  $l = 1$  to  $L$  do                         for  $l = L$  to  $0$  do  

     $\tilde{\mathbf{z}}^{(l)} \leftarrow \text{batchnorm}(\mathbf{W}^{(l)} \tilde{\mathbf{h}}^{(l-1)}) + \text{noise}$            if  $l = L$  then  

     $\tilde{\mathbf{h}}^{(l)} \leftarrow \text{activation}(\boldsymbol{\gamma}^{(l)} \odot (\tilde{\mathbf{z}}^{(l)} + \boldsymbol{\beta}^{(l)}))$             $\mathbf{u}^{(L)} \leftarrow \text{batchnorm}(\tilde{\mathbf{h}}^{(L)})$   

end for                                         else  

 $P(\tilde{\mathbf{y}} | \mathbf{x}) \leftarrow \tilde{\mathbf{h}}^{(L)}$             $\mathbf{u}^{(l)} \leftarrow \text{batchnorm}(\mathbf{V}^{(l+1)} \hat{\mathbf{z}}^{(l+1)})$   

# Clean encoder (for denoising targets)          end if  

 $\mathbf{h}^{(0)} \leftarrow \mathbf{z}^{(0)} \leftarrow \mathbf{x}(n)$             $\forall i : \hat{z}_i^{(l)} \leftarrow g(\tilde{z}_i^{(l)}, u_i^{(l)})$  # Eq. (2)  

for  $l = 1$  to  $L$  do                          $\forall i : \hat{z}_{i,\text{BN}}^{(l)} \leftarrow \frac{\hat{z}_i^{(l)} - \mu_i^{(l)}}{\sigma_i^{(l)}}$   

     $\mathbf{z}_{\text{pre}}^{(l)} \leftarrow \mathbf{W}^{(l)} \mathbf{h}^{(l-1)}$            end for  

     $\boldsymbol{\mu}^{(l)} \leftarrow \text{batchmean}(\mathbf{z}_{\text{pre}}^{(l)})$           # Cost function  $C$  for training:  

     $\boldsymbol{\sigma}^{(l)} \leftarrow \text{batchstd}(\mathbf{z}_{\text{pre}}^{(l)})$             $C \leftarrow 0$   

     $\mathbf{z}^{(l)} \leftarrow \text{batchnorm}(\mathbf{z}_{\text{pre}}^{(l)})$            if  $t(n)$  then  

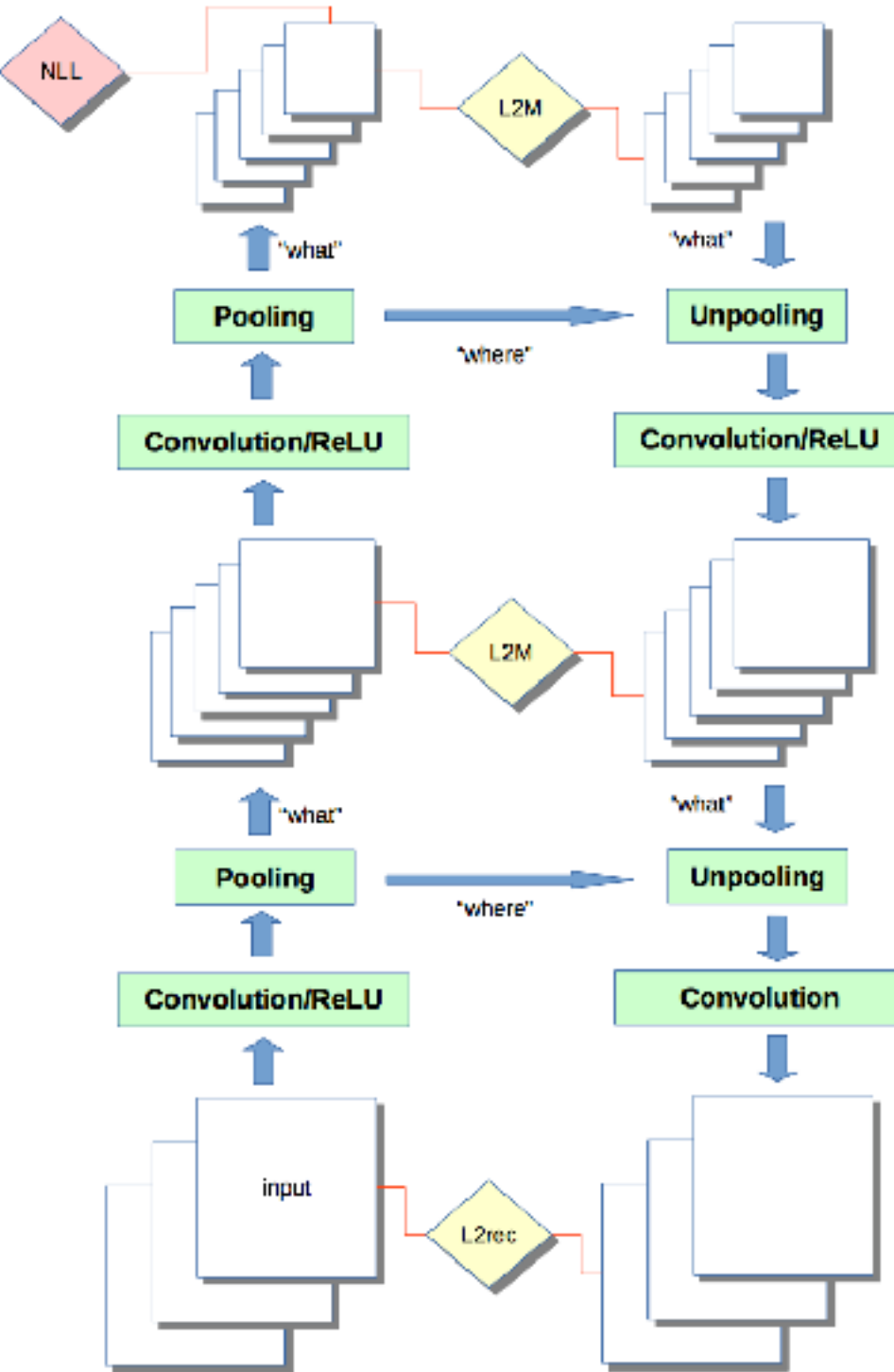
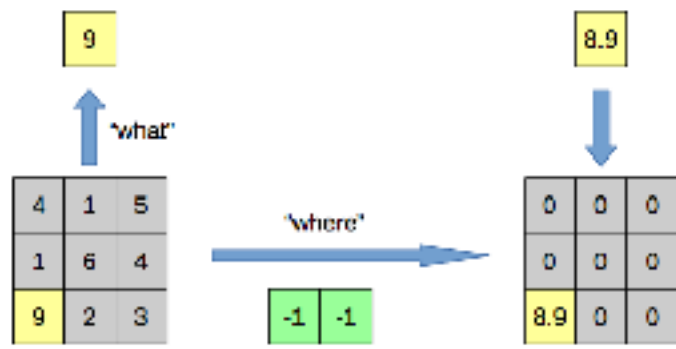
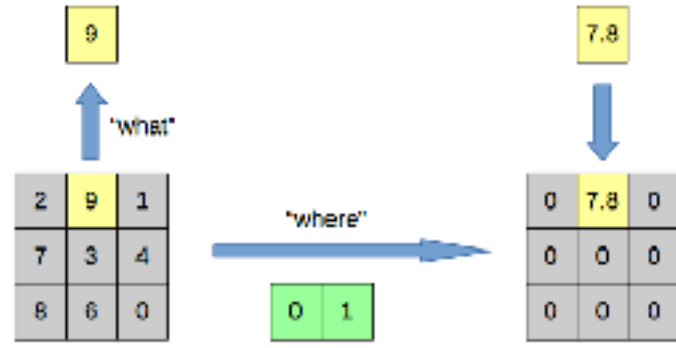
     $\mathbf{h}^{(l)} \leftarrow \text{activation}(\boldsymbol{\gamma}^{(l)} \odot (\mathbf{z}^{(l)} + \boldsymbol{\beta}^{(l)}))$             $C \leftarrow -\log P(\tilde{\mathbf{y}} = t(n) | \mathbf{x}(n))$   

end for                                         end if  

                                                 $C \leftarrow C + \sum_{l=0}^L \lambda_l \left\| \mathbf{z}^{(l)} - \hat{\mathbf{z}}_{\text{BN}}^{(l)} \right\|^2$  # Eq. (3)

```

# Stacked What-Where Autoencoder



# Semi-supervised Results

Model	Number of incorrectly predicted test examples for a given number of labeled samples			
	20	50	100	200
DGN [21]			333 $\pm$ 14	
Virtual Adversarial [22]			212	
CatGAN [14]			191 $\pm$ 10	
Skip Deep Generative Model [23]			132 $\pm$ 7	
Ladder network [24]			106 $\pm$ 37	
Auxiliary Deep Generative Model [23]			96 $\pm$ 2	
Our model	1677 $\pm$ 452	221 $\pm$ 136	93 $\pm$ 6.5	90 $\pm$ 4.2
Ensemble of 10 of our models	1134 $\pm$ 445	142 $\pm$ 96	86 $\pm$ 5.6	81 $\pm$ 4.3

Table 1: Number of incorrectly classified test examples for the semi-supervised setting on permutation invariant MNIST. Results are averaged over 10 seeds.

Model	Test error rate for a given number of labeled samples			
	1000	2000	4000	8000
Ladder network [24]			20.40 $\pm$ 0.47	
CatGAN [14]			19.58 $\pm$ 0.46	
Our model	21.83 $\pm$ 2.01	19.61 $\pm$ 2.09	18.63 $\pm$ 2.32	17.72 $\pm$ 1.82
Ensemble of 10 of our models	19.22 $\pm$ 0.54	17.25 $\pm$ 0.66	15.59 $\pm$ 0.47	14.87 $\pm$ 0.89

Table 2: Test error on semi-supervised CIFAR-10. Results are averaged over 10 splits of data.

# Design Principles for Convnets: A Summary